The final, published version of this article is available at https://doi.org/10.1016/j.jnutbio.2019.01.001

CSRP3 Mediates Polyphenols-Induced Cardioprotection In Hypertension

Carole Oudot[1], Andreia Gomes[2,3], Valérie Nicolas[4], Morgane Le Gall[5,6], Philippe Chaffey[5,6], Cédric Broussard[5,6], Giuseppe Calamita[7], Maria Mastrodonato[8], Patrizia Gena[7], Jean-Luc Perfettini[9], Jocelyne Hamelin[10], Antoinette Lemoine[10], Rodolphe Fischmeister[1], Helena L.A. Vieira[2,11], Claudia N. Santos[2,3], Catherine Brenner[1]

[1]*INSERM UMR-S 1180, Univ Paris-Sud, Université Paris Saclay, Châtenay-Malabry, France*

[2]*iBET, Instituto de Biologia Experimental e Tecnológica, Apartado 12, 2780-901 Oeiras, Portugal*

[3]*Instituto de Tecnologia Química e Biológica António Xavier, Universidade Nova de Lisboa, Av. da República, 2780-157 Oeiras, Portugal*

[4]*UMS-IPSIT, Univ Paris-Sud, Université Paris Saclay, Châtenay-Malabry, France*

[5]*Institut Cochin, INSERM U1016, CNRS UMR 8104, Université Paris Descartes Sorbonne Paris Cité, Paris, France*

[6]*Plate-forme Protéomique 3P5, Université Paris Descartes, Paris, France*

[7]*Department of Biosciences, Biotechnologies and Biopharnaceutics, University of Bari "Aldo Moro", Bari, Italy*

[8] *Department of Biology, University of Bari "Aldo Moro", Bari, Italy*

[9]*Institut Gustave Roussy, INSERM U1030, Univ Paris-Sud, Université Paris Saclay, Villejuif, France*

[10]*Inserm U1193, Univ Paris-Sud, Université Paris Saclay, Villejuif, France*

[11] *CEDOC, NOVA Medical School, Faculdade de Ciências Médicas, Universidade Nova de Lisboa, Campo dos Mártires da Pátria, 130, 1169-056, Lisboa, Portugal*

Keywords: berries, polyphenols, hypertension, cardioprotection, CSRP3, sarcomere

Correspondence: Dr C. Brenner
INSERM UMR-S 1180
5 rue JB Clément
92296 Châtenay-Malabry
France
Tel: + 33 1 46 83 52 42
E-mail: catherinebrenner@yahoo.com

Abstract

Berries contain bioactive polyphenols, whose capacity to prevent cardiovascular diseases have been established recently in animal models as well in human clinical trials. However, cellular processes and molecular targets of berries polyphenols remain to be identified. The capacity of a polyphenol-enriched diet (i.e. blueberries, blackberries, raspberries, strawberry tree fruits and Portuguese crowberries berries mixture) to promote animal survival and protect cardiovascular function from salt-induced hypertension was evaluated in a chronic salt sensitive Dahl rat model. The daily consumption of berries improved survival of Dahl/Salt Sensitive rats submitted to high salt diet and normalized their body weight, renal function and blood pressure. In addition, a prophylactic effect was observed at the level of cardiac hypertrophy and dysfunction, tissue cohesion and cardiomyocyte hypertrophy. Berries also protected the aorta from fibrosis and modulated the expression of Aquaporin-1, a channel involved in endothelial water and nitric oxide (NO) permeability. Left ventricle proteomics analysis led to the identification of berries and salt metabolites targets, including Cystein and glycin-rich protein 3 (CSRP3), a protein involved in myocyte cytoarchitecture. In neonatal rat ventricular cardiomyocytes, CSRP3 was validated as a target of a berries derived polyphenol metabolite, 4-methylcatechol sulfate, at micromolar concentrations, mimicking physiological conditions of human plasma circulation. Accordingly, siRNA silencing of CSRP3 and 4-methylcatechol sulfate pretreatment reversed cardiomyocyte hypertrophy and CSRP3 overexpression induced by phenylephrine. Our systemic study clearly supports that the modulation of CSRP3 by a polyphenol-rich berries diet as an efficient cardioprotective strategy in hypertension-induced heart failure.

1. Introduction

Hypertension is an important worldwide public-health challenge because of its high frequency and concomitant risks for cardiovascular and kidney disease [1]. According to the World Health Report 2002, 49% of ischemic heart disease are attributable to high systolic blood pressure (SBP) (SBP>115 mm Hg) levels, which is estimated to cause 7.1 million deaths worldwide. Hypertension promotes many deleterious changes in cardiac structure, such as left ventricle (LV) hypertrophy and decreased function, which progressively can cause heart failure [2,3]. During progression of the disease, the cytoskeleton remodels its architecture to adapt to extrinsic mechanical loads [4–6]. Among cytoskeletal proteins, cysteine and glycine-rich protein 3 (CSRP3) is essential for the maintenance of myocyte architecture and being a mechanosensor protein participating in the assembly of actin-based cytoskeleton through interaction with many cytoskeleton proteins [7-9]. In line with these observations, CSRP3-deficient mice develop a dilated cardiomyopathy with myocyte hypertrophy and heart failure [8], whereas cardiac overexpression of CSRP3 is not beneficial [10]. Importantly, in human, CSRP3 gene mutations lead to hypertrophic cardiomyopathy [11]. Thus, CSRP3 has recently emerged as a key regulator of cardiac pathophysiology [12], prompting us to hypothesize that the stabilization of CSRP3 protein expression could prevent the development of deleterious cardiac hypertrophy *in vitro* and heart failure *in vivo*.

Previously, the Dietary Approaches to Stop Hypertension (DASH) trial [13] and Lyon Diet Heart Study [14] demonstrated that a high daily intake of foods rich in polyphenols such as fruits and vegetables may have beneficial effects in humans *via* the decline of cardiovascular risk factors such as SBP [15–17]. Berries have received attention for preventing and control cardiovascular diseases due to their considerably high concentrations of flavonoids. Nevertheless, the underlying mechanisms of berries-derived polyphenols have been mostly assessed by using total extract or pure derived compounds on tissue or cell culture; without considering their metabolization and bioavailability, which strongly limits the physiological impact of the study. Circulating polyphenol metabolites from berries have been recently

identified by our group in human plasma and urine and pharmacokinetic parameters such as, physiological plasma concentrations and time of circulation in human body of these metabolites were determined [18,19]. This allows us to design preclinical cellular studies with physiologic concentrations of relevant polyphenols metabolites (e.g. 4-methylcatechol sulfate, a representative metabolite of berries's polyphenols detected in circulation) for human health [18]. Moreover, prompted by independent studies showing a potential role of resveratrol on the heart [20,21] this compound was also evaluated in cells.

Overall this study aimed at demonstrating the role of a polyphenol-enriched diet on hypertension-induced heart failure progression using the Dahl-Salt Sensitive (Dahl/SS) rat model, which is a well-established preclinical chronic model that provides insights into the pathology and treatment of salt sensitive hypertension [22,23]. We observed positive effects at the level of the heart, as well as the kidney and the aorta. Furthermore, we performed a global proteomic study *in vivo* of the identified LV proteins implicated in hypertrophy and cardioprotection. Berries diet improved dramatically animal survival, decreased hypertension and cardiac hypertrophy and enhanced cardiac function *in vivo*. Finally, based on pharmacological, genetic and cellular experiments in primary cardiomyocytes, CSRP3 emerged as a key protein mediating the protective cardiac effects of berries derived metabolites *via* an impact on tissue cohesion maintenance and hypertrophy.

2. Methods

Unless specified, reagents are from Sigma Aldrich, Saint Quentin Fallavier, France.

2.1. Animal care and diets

All animal care and experimental procedures were performed according to the European Community guiding principles in the care and use of animals (Directive 2010/63/EU of the European Parliament) and authorizations to perform animal experiments according to this directive were obtained from the French Ministry of Agriculture, Fisheries and Food (No. D-

92-283, 13 December 2012, N°APAFIS#2152-2015092912128144 v3). All studies involving rats are reported in accordance with the ARRIVE guidelines for reporting experiments involving animals.

Five-week-old male Dahl/SS rats were obtained from Charles River (L'Abresle, France) and were acclimated for 1 week on AIN-76A powder diet (INRA UPAE, Jouy-en Josas, France). After this period, rats were randomly assigned two per cage for 10 weeks to one of four treatments: low salt diet (LS, 0.26% NaCl), LS (0.26% NaCl) + berries mixture powder (LS Berries, 2g/day), high salt diet (HS, 8% NaCl), HS + berries mixture powder (HS Berries, 2g/day). AIN-76A diets with LS or HS content were manufactured by INRA UPAE. Diets nutrient content is described in Table Supp 1. The berries powder was prepared as described below. Berries powder was mixed with AIN-76A ± salt-containing diets and frozen for less than 2 days until use. Rats were housed in climate-controlled conditions with a 12h light/dark cycle in a temperature-controlled room (22±1°C). Water was given *ad libitum*.

2.2. Preparation of the berries mixture

The mixture of five different berries consisted in: blueberries (*Vaccinum* spp. variety Georgia Gem), blackberries (*Rubus* L. subgenus Rubus Watson variety Karaka Black) and raspberries (*Rubus idaeus* L. variety Himbo Top) harvested at the Fataca experimental field in Odemira, Portugal; strawberry tree fruits (*Arbutus unedo* L.) harvested in the Alentejo region, Portugal, and Portuguese crowberries (*Corema album* L.) harvested in the Comporta region, Portugal. Berries were blended together using a domestic food processor at room temperature. The resulting puree was freeze-dried to powder and stored at −80ºC in the dark until further use. The berries mixture polyphenol content was estimated before and after inclusion in diets according to the Folin−Ciocalteau method adapted for microplates. Gallic acid was used as standard, and the results were expressed in milligrams of gallic acid equivalents per g of berries mixture (mgGAE/g dw). It was estimated a daily dose of 67 mgGAE per 2g of the berries mixture supplemented in the diet. It was confirmed that AIN-76A powder diet did not change the contribution to the content in polyphenols. Moreover

polyphenol profile of the berries mixture is in compliance with the chemical characterization already described by us for the same fruits and mixture [18].

2.3. Blood pressure measurements

At 3, 6 and 9 weeks, systolic BP (SBP) was measured in conscious, restrained rats using tail-cuff system (CODA, EMKA Technologies France). Rats were subjected to five measurements of preconditioning. After preconditioning, the first ten of twenty measurements were systematically discarded because of the BP variability due to acclimatization to the tail cuff pressure, the box and operational noise. A run was accepted if at least six or ten measurements were obtained. The mean systolic SBP value was calculated on two runs at one day-interval.

2.4. Echocardiography

LV function and structure were assessed by serial transthoracic echocardiography using a 12 MHz transducer (Vivid 7, General Electric Healthcare) under 2.5% isoflurane gas as anesthesia. Parasternal long axis and short-axis M-mode tracings of the left ventricle (LV) were recorded at the level just above the papillary muscles, and LV end-diastolic diameter (LVDd), LV end-systolic diameter (LVSd), interventricular septum thickness (IVSd) and LV end posterior wall thickness (PWd) were measured. Relative wall thickness (RWT) was calculated using the formula (PWd+IVSd)/LVDd. LV fractional shortening (LVFS) was calculated using the equation: 100 × ((LVDd−LVSd)/LVDd). LV ejection fraction (LVEF) was calculated similarly but using the volumes instead of the diameters. LV end-systolic volume (LVSV) and end-diastolic volumes (LVDV), as well as ejection fraction, were obtained automatically on the echocardiograph according to the Teichholtz formula $LVSV=7x\ LVSd^3/2.4+LVSd$ and $LVDV=7xLVDd^3/2.4+LVDd$. The ratio of peak early-filling velocity of transmitral flow (E) to the corresponding mitral valve annulus velocity (E') was evaluated. All measurements were averaged from three consecutive cardiac cycles under stable

conditions. LV mass was calculated according to the Penn formula home adapted for the rat heart: (LV mass =1.04x[(LVDd+SIVd+PWd)^3-(LVDd)^3]).

2.5. Terminal plasma analysis

At the end of the study, conscious rats were decapitated to avoid anaesthetic interference with biochemical analysis and collected as indicated in the ethical protocol (N°APAFIS#2152-2015092912128144 v3). Blood was collected in heparin and then spun at 4°C, 5000 x *g* for 20 minutes.The plasma was collected and stored at – 20°C until further analysis. Cholesterol and triglycerides were measured by Abbott *Architect c8000 (Abbott, Rungis, France).* Fasting glucose was instantly obtained on Alere *Cholestech LDX® analyser* (Gaïamed, *Boulogne* Billancourt*,* France).

2.6. Metabolic parameters

The last week of the trial, all rats were housed in individual metabolic cages and body weight, food, and water consumption, as well as urinary excretion of water, sodium, and potassium were measured daily for three days. For metabolic analysis, rats were fasted overnight. Organ weights (heart, lungs, kidney and liver) were compared to tibia length rather than to body weight, because of the variable weight loss from cachexia. Heart chambers were isolated and cut. One biopsy of LV was fixed in formalin and two remaining biopsies were frozen in liquid nitrogen and stored at -80°C until further use.

Urine and plasma concentration of sodium, potassium and creatine were measured with Abbott Architect c8000 (Abbott, Rungis, France)

2.7. Cardiac and aorta tissue analysis

Cardiac and aorta tissues were analyzed by histology and immunohistochemistry, respectively as described below.

2.7.1. Cardiac tissue

Formalin-fixed LV section were embedded in paraffin, cut into 6-µm sections and mounted on slides. To investigate the cardiac fibrosis, LVs from five rats per group were stained with Masson's Trichrome stain and analyzed [25]. Five to eight fields per LV were analyzed and data were expressed as a percentage of the total area of the field. Collagen was measured by color-deconvolution of images from Masson-trichrome stained left ventricle sections. Threshold in Image J was applied. Area percentage of collagen was obtained by division of the combined image by the total tissue image.

To investigate the cardiac remodeling, inflammation [26] and sarcomere organization, 6-µm-thick sections of LV from five rats per group were stained with hematoxylin and eosin [26]. To estimate inflammation, blind histological grading was performed on epicardium. Total images (15-30 images by rat group) were based on three semi-quantitative categories: no inflammation; minimal inflammation; moderate to severe inflammation. Total images from endocardium (15 to 30 images) by rat group were analyzed for the sarcomere organization using also three semi-quantitative categories. Sarcomerization was performed rating cardiomyocytes as having parallel bundles (no sarcomerization desorganization) or minimal desorganization (1 to 5 desarcomerized cardiomyocytes by image) or moderate to severe desarcomerization (more than 5 desarcomerized cardiomyocytes by image). To evaluate cardiomyocyte area, five images from endocardial LV were analyzed with ImageJ software (National Institute of Health).

2.7.2. Aorta tissue

Formalin-fixed thoracic aortas were embedded in paraffin, cut into 6-µm sections, and mounted on slides. These sections were staining with 0.1% Sirius red [27]. For immunohistochemistry assays the sections were incubated with antibody conjugated with fluorescein isothiocyanate (FITC) or peroxidase, anti-peroxidase (PAP) method. For the FITC immunofluorescence assay, the sections were treated with the blocking buffer containing 1% normal goat serum in phosphate-buffered saline (PBS) for 30 min at room temperature and incubated overnight with a rabbit anti-aquaporin 1 (AQP1) primary antibody (Proteintech, Rosemont, IL, USA) diluted 1:100 in blocking buffer at 4°C. After several rinses in PBS,

sections were incubated with the secondary antibody, *i.e.*, anti-rabbit Alexa Fluor 488 (Molecular Probes, Eugene, OR, USA) diluted 1:20 for 1 h at room temperature. After several washes in PBS, sections were finally mounted with N-propyl gallate in 50% glycerol.

For the PAP immunohistochemistry assay, the endogenous peroxidase was blocked by incubating sections in PBS containing 1% H_2O_2 for 10 min at room temperature. After several washes in PBS, the sections were treated with the blocking buffer with 1% normal goat serum in PBS for 30 min at room temperature and incubated overnight with a rabbit anti-AQP1 primary antibody (Proteintech) diluted 1:100. After several rinses in PBS, sections were incubated with the secondary antibody anti-rabbit IgG diluted 1:20 in blocking buffer for 1 h at room temperature. After several washes in PBS, sections were incubated with horseradish PAP complex at a dilution of 1:100 for 1 h at room temperature. Finally, immunolabelling was visualized by incubation with 3-3'-diaminobenzidine/H_2O_2 medium for 10 min at room temperature. Finally, the sections were dehydrated and mounted with Entellan (Merck, Darmstadt, Germany). The images were captured using an epifluorescence E600 photomicroscope equipped with a DMX 1200 digital camera (Nikon Instruments SpA, Calenzano, Italy). Negative controls were performed by omitting the primary antibodies or using antibodies pre-adsorbed with the immunizing peptide. Following Sirius staining of the aorta, the inner and outer circumference of the tunica media was manually traced with ImageJ software, and the internal and external cross-sectional areas were recorded. The area inside each respective perimeter was determined, and the difference between these areas was reported as the aortic cross section area.

2.8. Primary neonatal rat ventricular cardiomyocytes isolation, culture and siRNA treatments

Neonatal rat ventricular cardiomyocytes (NRVCs) were obtained from neonatal Wistar rats (2–3 days old) as previously described [28]. For western-blot, freshly isolated cardiomyocytes were plated in 6 well-plates manually coated with 0.1% gelatin at a density of $2x10^6$ cells. Alternatively, cardiomyocytes were plated on 35 mm dishes coated with

0.05mg/ml poly-D-lysine and 0.05% gelatin at a cell density of $2x10^6$ cells per dish for analyses on live cells with 4 µM calcein (calcein AM, Life technologies, St Aubin, France) and at 0.5 x 10^6 cells for immunostaining. Initially, cells were grown in DMEM (Gibco) containing 5% new born serum, 1% glutamine and 1× antibiotics (Gibco) for 24 hours. The day after, cells were transfected with 80 nM siRNA CSRP3 or control sRNA (GE Healthcare, Velizy-Villacoublay, France) using Lipofectamine RNAiMAX transfection (Fisher scientific, Illkirch, France) reagent in OptiMem (Life technologies) during 18h. During the last 48h, cells were transferred to serum-free medium in presence or absence of 50 µM phenylephrine alone or pre-incubated for 2h with various doses of 4-methylcatechol sulfate (1, 5 and 10 µM) and as a positive control resveratrol (5 and 10 µM). 4-methylcatechol sulfate was chemically synthetized as previously described [19].

2.9. Immunohistochemistry

After treatments, cells for immunostaining were washed with PBS and fixed with 4% formaldehyde. Triton X-100-permeabilized cells were incubated with anti α-actinin antibody (1:800) or CSRP3 antibody (1:200, Interchim, Montluçon, France). Cells were then incubated with respectively AlexaFluor goat anti-mouse secondary antibody (ThermoFisher scientific, Courtaboeuf, France), or AlexaFluor anti-rabbit secondary antibody (ThermoFisher scientific) and viewed under a fluorescent microscope in inverted confocal laser scanning microscope LSM 510-Meta (Carl Zeiss, Germany) using a Plan-Apochromat 63X/1.4 objective lens, equipped with an argon (488 nm excitation wavelength) and a helium neon laser (543 nm excitation wavelength).

To evaluate cardiomyocyte staining with anti α-actinin or CSRP3 antibodies, 5 images by group were analyzed with ImageJ software (National Institutes of Health).

To evaluate cardiomyocyte volume on live cells, NRVCs were pre-incubated with calcein AM for 10 min at 37°C and observed under fluorescent microscope (as described above). 5 images by group and 5-10 cells per images were analyzed with ImageJ software.

2.10. Western Blot

For protein extraction, neonatal rat ventricular cardiomyocytes were washed twice with PBS and lysed in HEPES buffer (50mM HEPES, 50mM KCL, 1 mM EDTA, 1mM EGTA, 5mM Beta-glycero-Phosphate, 0.10% Triton (pH 7.6) containing protease and phosphatase inhibitor (left ventricule tissue were lysed with RIPA buffer 1X (50mM Tris, 50mM NaCl, 1mM EDTA, 0.5% deoxycholate, 1% Triton X100, 0.1% SDS (pH 8.0) containing protease and phosphatase inhibitors. Snap-frozen ventricular tissues were minced and homogenized in radioimmunoprecipitation assay buffer (RIPA) with a Bead Beater (Bertin Technologies Precellys 24). All lysates were cleared by centrifugation at 12 000 x *g* for 30 min at 4°C. Supernatants were kept for the protein expression analysis. Protein concentration was determined using a Bicinchoninic acid (BCA) Protein Assay Kit. Protein samples were prepared by mixing protein samples in 1× Laemmli buffer, followed by heating the samples at 90°C for 10 minutes.

CSRP3 (Interchim), sarcomeric α-actinin (Sigma), Beclin (Cell Signaling, Paris, France), Apoptosis inducing factor (AIF) (Santa Cruz Biotechnology, Saint Quentin, France), Caspase 3 (Santa Cruz Biotechnology), poly(ADP-ribose) polymerase *(*PARP*)* (Santa Cruz Biotechnology), cytochrome *c (*BD Biosciences*,* St Quentin Fallavier*,* France*)* and glyceraldehyde-3-phosphate dehydrogenase (GAPDH) (Cell Signaling) expression in LV tissues and in cells were evaluated using immunoblot analysis. Proteins were resolved on 8 or 12% SDS-PAGE gels and electroblotted onto polyvinylidene fluoride (PVDF) membranes (Bio-Rad, Marnes La Coquette, France). Following electrotransfer, membranes were blocked for 1 h at room temperature in 5% BSA-PBST (10 mM Tris-HCl, pH 8.0/150 mM NaCl/0.1% Tween 20). Membranes were then incubated overnight at 4°C with primary antibodies against CSRP3 (1:1000), α-actinin (1:2000), Beclin (1:1000), AIF (1:500), Caspase 3 (1:1000), PARP (1:1000), cytochrome *c* (1:1000) and GAPDH (1:2500). On the following day, membranes were washed three times with PBST and incubated with peroxidase-conjugated secondary antibody at room temperature for 1 h. Peroxidase activity was detected with enhanced chemiluminescence (ECL Advance Western blotting detection kit; Thermo

Scientific, Villebon sur Yvette, France). Protein contents were expressed as a ratio relative to the loading control GAPDH.

2.11. Proteomic Analysis

Proteomic analysis included a tissue sample preparation to extract protein, then two-dimensional difference in gel electrophoresis (2D-DIGE) followed by protein identification by mass spectrometry (MS). To ensure reliability, all samples from the four rat groups were processed simultaneously.

2.11.1. Tissue sample preparation

The frozen cardiac LV (n=3 rats per group) were individually pulverized under liquid nitrogen to yield a fine powder using a pestle and a mortar. The tissue powder was solubilized in 15 volumes of lysis buffer (8 M urea, 2 M thiourea, 4% CHAPS, 60 mM dithiothreitol (DTT)). Then the protein extracts were clarified by ultra-centrifugation at 100,000x*g* for 1 h at 4°C. The supernatants were then treated with the 2D Clean-Up kit (GE Healthcare, Velizy-Villacoublay, France) according to the manufacturer's instructions. The resulting dry pellets were resuspended in lysis buffer without DTT and adjusted to pH 8.5 with 1.5 M Tris-base. Protein concentrations of the samples were determined by the Bradford method, and were in the range of 9–20 g/L.

2.11.2. Two-dimensional difference in gel electrophoresis (2D-DIGE)

The LV samples (50 µg) labelling with CyDyes™Fluor minimal dyes (GE Healthcare) and 2D-electrophoresis were done as previously described [29].

Image analysis, relative quantification, statistical evaluation and PCA (Principal Component Analysis) were carried out with DeCyder™ 2D software (GE Healthcare, version 7.2). The fold change (Fc) and Student's *t*-test *p*-values were calculated across several pairwise comparisons (HS *vs.* LS; HS Berries *vs.* HS; LS Berries *vs.* LS) and considered significant for p values < 0.05 and Fc ≥ 1.3 or ≤ 1.3.

2.11.3. Protein identification by mass spectrometry (MS)

Proteins in spots of interest were identified by mass spectrometry. In-gel digestion was carried out with trypsin (12.5 ng/µL in 40 mM NH_4HCO_3–10% acetonitrile (ACN), overnight at 37°C) as described by Shevchenko *et al*. [30] with minor modifications and using Freedom EVO 100 digester/spotter robot (Tecan, Männedorf, Switzerland).

MS and MS/MS analyses were performed using an Ultimate 3000 Rapid Separation Liquid Chromatographic (RSLC) system (Thermo Fisher Scientific) online with a hybrid LTQ-Orbitrap–Velos mass spectrometer (Thermo Fisher Scientific). Briefly, after trypsin digestion peptides were loaded and washed on a C_{18} reverse-phase precolumn. The loading buffer contained 98% H_2O, 2% ACN, and 0.1% trifluoroacetic acid (TFA). Peptides were then separated on a C_{18} reverse-phase resin with a 4 min effective gradient from 100% solvent A (0.1% formic acid and 99.9% H_2O) to 50% solvent B (80% ACN, 0.085% formic acid, and 20% H_2O).

The linear trap quadrupole-Orbitrap mass spectrometer acquired data throughout the elution process and operated in a data-dependent scheme, with full MS scans acquired with the Orbitrap mass spectrometer, followed by the acquisition of up to 20 LTQ MS/MS collision-induced dissociation spectra on the most abundant ions detected by the MS scan. Mass spectrometer settings were as follows: for full MS, automatic gain control (AGC) was $1x10e^6$, the resolution was $6x10e^4$, the m/z range was 400 to 2,000, and the maximum ion injection time was 500 ms; for MS/MS, AGC was $5x10e^3$, the maximum injection time was 50 ms, the minimum signal threshold was 500, the isolation width was 2 Da, and the dynamic exclusion time setting was 15 s. Precursors were fragmented with charge states of 2, 3, and 4. The signal-to-noise threshold for extraction values was 3.

Database searches were carried out using the Mascot server (version 2.4; Matrix Science, London, United Kingdom) on rattus from the Swiss-Prot databank (7,932 sequences, February 2015, www.expasy.org). The search parameters were as follows: carbamidomethylation as a variable modification for cysteines and oxidation as a variable

modification for methionine. Up to one missed tryptic cleavage was tolerated. The mass accuracy tolerance for all tryptic mass searches was 5 ppm for precursors and 0.56 Da for fragments. Positive identification was based on a Mascot score above the significance level (*i.e.* <5%). The reported proteins were always those with the highest number of peptide matches. With our identification criteria, no result was found to match multiple members of a protein family.

2.12. Statistical analysis

All values are expressed as mean±SEM. The Statistica software (StatSoft, Inc, Tulsa, OK, USA) was used for statistical analysis. Kaplan-Meier survival curves for the rats were constructed and compared with the logrank test.

For analysis on tissue and for echocardiography, comparisons between 3-4 groups were performed with a one-way ANOVA followed by *post hoc* F-Fisher test and 2 groups comparison with Student *t* test. For cellular analysis, we choose significance Kruskal Wallis test and Mann-Whitney test for 2 groups comparison. Chi2 followed by a Fisher's exact test was used for inflammation and desarcomerization evaluation. In 2D-DIGE experiments, protein content was compared with ANOVA test (gate keeper strategy). When relevant, the Tukey's multiple comparison test was used to investigate between which groups the difference in protein expression is significant. Tests were used to compare groups and a protein spot with a score of fold change (Fc) ≥1.3 or ≤-1.3 with $p<0.05$ was considered as differentially-expressed and statistically significant. The number of animals, cells, groups and independent experiments performed are indicated in the figure legends.

3. Results

3.1. Berries consumption improved rat survival, weight and blood pressure in Dahl/SS rat chronic model of hypertension

To investigate the capacity of berries mixture to protect Dahl/SS rat from salt-induced cardiovascular damage, rats were fed with a low salt (LS) diet (0.26% NaCl) or high salt (HS)

diet (8% NaCl) and diet supplemented with berries (2g/day/animal, LS Berries or HS Berries) or not for 10 weeks as described in Fig 1A using supplemented AIN-76A diet (Table Supp 1). As expected, no animals from LS and LS Berries groups died during the trial. In the HS group, mortality reached 40%, rats dying predominantly from stroke (Fig 1B). A positive effect of berries-enriched diet on survival became statistically significant from 6 weeks (p<0.05) until the end of the study, leading to 30% lower animal death in the group with HS diet supplemented with berries (p<0.05). During the study, no significant differences either in survival rate or body weight gain were observed between LS and LS Berries rats (Fig 1B and 1C). In contrast, we observed a significant loss of body weight in the HS rats from 6 weeks (Fig 1C). The weight loss was significantly prevented by berries consumption until the end of the trial (Fig 1C). It was due to a decrease in food consumption of HS rats, but not to an increased excreted volume of urine since there was not difference between HS and HS berries rats urinary volume (Table Supp 2).

Fig 1D shows that systolic blood pressure (SBP) in HS rats was substantially higher compared to LS animals at 3, 6 and 9 weeks, confirming the deleterious effect of salt on SBP and validating the experimental hypertension model. The SBP of LS berries rats tended to be higher at 6 weeks but normalized at 9 weeks in comparison to LS rats. Interestingly, berries alleviated the development of hypertension induced by HS diet after 3 and 6 weeks. However, SBP of HS rats decreased at 9 weeks and, thereby, reached the level of HS Berries rats (Fig 1D), indicating that hypertension is not the only parameter responsible for the deleterious effect of HS treatment (see below). Taken all together, the results show that HS diet promotes animal death, decreases body weight and increases hypertension, while consumption of berries reverted these deleterious events. Thus, our berry-enriched diet presented cardiovascular beneficial properties.

3.2. Influence of high salt diet and berries on metabolic and biochemical parameters

At 9 weeks, HS diet increased water intake by the rats, irrespective of berries addition into the food (Table Supp 2). Whether excreted urinary volume are similar between HS and HS berries rats, sodium intake increased in HS group (p<0.05), its levels being much higher in HS Berries group (p<0.05) in line with increased food consumption (Table Supp 2). ANOVA analysis demonstrated that total plasma cholesterol concentrations and HDL-cholesterol concentrations (data not shown) were overall not significantly affected by dietary sodium content (Fig 2A). Triglyceride concentrations were also unaffected by diet in all three strains (Fig 2B).

3.3. Berries prevented cardiac hypertrophy and protected cardiac function

Echocardiography was used to assess cardiac function (Fig 1E and Table Supp 3) and measurements of anatomical parameters (Fig 1E and Table Supp 4). There were no differences in heart parameters and cardiac function between LS and LS Berries rats (Fig 1E and Table Supp3) and some significant changes between LS berries, HS and HS berries depending on the parameter. Additionally, no change in heart rate between the four groups of rats was found (Table Supp 3).

The HS diet significantly induced cardiac hypertrophy, which was observed *via* echocardiographic and post-mortem analyses, as indicated by significant increase in LV weight/tibia length (0.29 ±0.02 *vs* 0.20±0.01, HS *vs* LS (p<0.05)) (Fig 1E) and relative wall thickness (RWT) (p<0.05). Within other parameters of LV remodeling, LV end-systolic diameter (LVSd), the posterior wall thickness at end diastole (PWTd) were also significantly increased in HS group compared to LS group (p<0.05) (Fig 1E, Table Supp3). In addition, the Doppler analysis showed that HS rats had a decreased filling function as indicated with E' index (4.1±0.8 *vs* 7.1±1.6, HS *vs* LS, p<0.05) and a significantly increase in filling pressure (17.7±5 *vs* 14.0±3.1, HS *vs* LS, p<0.05) as indicated with E/E' (Table Supp 3).

Berries ingestion reduced the cardiac hypertrophy in HS rats (p<0.05, Fig 1E) and prevented the increase in LVSd (p<0.05, Fig 1E), maintaining the relative wall thickness (RWT) unchanged (p<0.05) (Table Supp 3). These beneficial structural changes induced by berries

in HS rats were accompanied by a significant increase in functional cardiac parameters such as LV ejection fraction (LVEF, $p<0.05$, Table Supp 3) and LV fractional shortening (LVFS, $p<0.05$, Fig 1E). However, HS Berries rats had a lesser decrease of filling function than HS rats as shown by the Doppler analysis ($p<0.05$, Table Supp 3). In conclusion, these data revealed that berries ingestion prevented most of the cardiac structural and functional changes induced by the high salt diet.

3.4. Berries induced left ventricle tissue protection

Histological analysis showed that HS diet induced an increase in cardiomyocyte cell surface area (Fig 2A). Interestingly, HS Berries diet inhibited cardiomyocyte hypertrophy induced by the salt ($p<0.05$, Fig 2A). Figure 2B shows that HS group developed a regionalized desarcomerization, *i.e.* a disorganization of the endocardium tissue, ranging from 10% for minimal desarcomerization to 54% for moderate to severe grade. HS Berries prevented this loss of tissue cohesion, with a decrease of 9% for moderate to severe grade. In contrast, the epicardium showed no modification of loss of cytoarchitectural organization (Fig 2C). Moreover, HS rats showed epicardium inflammation, ranging from 30% for minimal inflammation to 57% for moderate to severe grade (Fig 2C), with the hematoxylin/eosin staining revealing an increase in invaded inflammatory cells detected as brown cells (Fig 2C). On contrary, in LV from HS Berries, inflammation levels decreased, namely from 57% in HS to 23% in HS Berries. Despite the fact that HS diet was associated with a significant increase in vascular collagen deposition without significant interstitial fibrosis (Fig 2D), the HS Berries diet did not modify this effect. In summary, berries consumption limited inflammation, tissue disorganization and loss of LV cytoarchitecture occurring in rats that consumed a high salt diet.

3.5. Berries-enriched diet promoted beneficial systemic effects

Next, we addressed systemic effects of berries on other organs targeted by hypertension, such as aorta and kidney that could impact indirectly on the heart [31,32]. Thus, berries

decreased significantly the aortic wall cross section in HS Berries rats in comparison with the HS group (1093±163 μm^2 *vs* 1290±81 μm^2) close to the level in LS rats (882±64 μm^2) (Fig 3A, B). Moreover, berries consumption restored the expression of Aquaporin-1 (AQP1), an endothelial membrane channel conducting NO in addition to water [33,34], which was decreased in HS rat (Fig 3C). In addition, beneficial effects of berries on kidney were observed, with a decrease in kidney weight (Table Supp4) and function in comparison with the rats in a HS diet as shown by differences in terms of creatinuria and renal clearance (Table Supp 2). Of note, no significant change in lung weight between HS and LS was observed (Table Supp4) correlating with an absence of lung edema and congestion and an early stage of HF. These results indicate that berries had concomitant protective effects on other organs than the heart.

3.6. Molecular mechanisms of the cardioprotective effects of berries

To get some insight into the molecular mechanisms underlying the beneficial role of berries on the cardiovascular system, we sought to determine the LV global proteome changes induced by HS diet and berries in the Dahl/SS rats (Fig 4). Using 2D-DIGE approximately 2000 spots per gel were detected, matched and compared between the 4 experimental groups (LS, LS Berries, HS and HS Berries). Proteomic analysis revealed that 52 spots were differentially expressed between the groups and identified by liquid chromatography-mass spectrometry/mass spectrometry (LC-MS/MS) (Fig 4A-C and Table Supp 5). All these 52 spots corresponding to 37 proteins were differentially expressed between HS and LS rats (Fig 4 and Table Supp 5), meaning that these protein changes result from the salt consumption. Berries modified expression of only 14 spots corresponding to 8 proteins ($p<0.05$) in HS fed rats (Fig 4, Table Supp 5 and Table Supp 6).

No protein was differentially expressed between LS and LS Berries (Table Supp 5). Principal component analysis (PCA) and hierarchical clustering analysis (HCA) of the 52 differentially expressed spots clearly distinguished LS and HS group (Fig 4B). Whereas the effect of

berries consumption was clearly identified in rats fed with HS diet, this was not observed in the groups fed with a LS diet (Fig 4B).

The differentially-expressed proteins belong to the following pathways: metabolism regulation, muscle development and contraction, endoplasmic reticulum stress and cell homeostasis (Table Supp 5, Table Supp 6). In particular, CSRP3, which is a key protein in the maintenance of myocyte cytostructure and cardioprotection, was found to be differently expressed. Indeed, HS-induced pressure overload significantly increased CSRP3 expression by 2.0-fold compared to LS diet fed rats, whereas berries counteracted this change (Table Supp 6). Thus, fold change of CSRP3 in HS Berries fed group *vs.* HS fed group was estimated at 1.3 (Table Supp 5, Table Supp 6). The CSRP3 protein changes were confirmed also by western-blot analysis of LV samples collected from animals (Fig 4D). An increase of 2.4-fold was determined between LS and HS rats, while in berries fed HS rats the expression level of CSRP3 was similar to LS rats (Fig 4D). Moreover, a contractile protein, myosin 7, was identified in several spots, suggesting variations in the post-translational processing of the protein. In contrast to mitochondrial adenylate kinase 2, which is down-regulated in HS and normalized in HS berries fed rats, major vault proteins - protein S100-A10, 78kDa glucose-regulated protein (GRP78), myosin 6 and 7, translocon-associated protein subunit delta - were up-regulated in HS rats *vs.* LS (Table Supp 6).

Intermediate metabolism and mitochondrial proteins such as β-enolase, cytochrome *c* oxidase subunit 5A, cytochrome *c* oxidase subunit 7A2, ATP synthase subunit e, ATP synthase subunit g, and very long chain specific acyl-coA dehydrogenase decreased in HS diet fed group, but it is worth noting that these proteins were not restored in HS Berries group (Table Supp 6). In addition, there was no change in mitochondrial mass in the four groups, as shown by citrate synthase activity measurement (Fig 5A).

Gene ontology (GO) analysis points only to Annexin A5 in terms of regulatory protein of apoptosis process (Table Supp 6) changing between HS and LS, but not between HS and HS HS Berries fed rats suggesting a minor implication of cell death in the salt-induced pathology. In the same line, no modification for cytochrome *c,* AIF, PARP (not shown) and

caspase 3 (not shown) in HS *vs* HS Berries groups by western-blot was observed (Fig 5B-C). This was in agreement with an absence of detectable apoptosis by immunostaining of HS and HS Berries LV sections (data not shown). Of note, only a minor decrease in autophagic proteins, LC3II and Beclin, in HS Berries was observed in comparison to HS fed rats, but the changes were not statistically significant (Fig 5D). These data revealed that the berries-elicited cardioprotective effects involved the modulation of an unexpected limited set of proteins and cellular processes, mainly by up-regulation, in particular CSRP3 expression, making of this protein a potential target for cardioprotective strategies.

3.7. CSRP3 siRNA modulates the degree of cardiomyocyte hypertrophy

Based on the histochemical analysis of LV tissue integrity (Fig 2) and proteome variation (Fig 4), we hypothesized that CSRP3 might be involved in the maintenance of intracellular architecture and cell size. To check that hypothesis, NRVCs were treated with 50 µM phenylephrine (PE) for 48h and the level of CSRP3 expression was measured by western-blotting (Fig 6A). PE treatment increased CSRP3 expression ~1.8-fold in parallel with a 3-fold increase in α-actinin, a cytoskeletal actin-binding protein considered as a hypertrophy marker (Fig 6A). These effects were blunted by siRNA-mediated knockdown of CSRP3. Likewise, quantification of the cell volume showed a significant (+1.5 fold) increase in the size of PE-treated *vs.* control cardiomyocytes that was prevented by CSRP3 down regulation (Fig 6B). Moreover, α-actinin immunodetection revealed larger cells with sarcomeric rearrangement in PE treated *vs.* control cardiomyocytes (Fig 6C), a phenomenon which was also significantly decreased with siRNA CSRP3 (Fig 6C). Altogether, the results suggest that α-actinin-mediated cytoorganization upon adrenergic stimulation partially depends on CSRP3 levels.

The final step was to examine whether CSRP3 was a target of berries-derived polyphenol metabolite. For this, NRVCs were exposed to the human bioavailable polyphenol metabolite 4-methylcathecol sulfate (MC) found in human healthy subjects consuming the same berry mixture as the rats in this study [19]. Pretreatment of cardiomyocytes for 2h with 5 or 10 µM MC decreased PE stimulation of CSRP3 expression (Fig 6D) and reduced in a dose-

dependent manner the PE-induced α-actinin expression (Fig 6D). Similar effects were observed with our positive control, resveratrol, for the same concentrations in reducing CSRP3 expression under PE stimulation (Fig 6E) and cardiomyocyte cell size (Fig 6B). Collectively, these results demonstrate that a berry-derived polyphenol metabolite can prevent hypertrophic responses in PE-stimulated cardiomyocytes, hence mimicking siRNA–mediated CSRP3 down-regulation.

4. Discussion

This study demonstrates, for the first time, the beneficial effects of polyphenol-enriched diet ingestion in a chronic model of hypertension-induced heart failure. Moreover, it identifies CSRP3 as a potential target in cardioprotection by modulating cardiomyocyte hypertrophy and cardiac tissue cohesion. The underlying molecular mechanisms and the role of CSRP3 were validated in primary neonatal rat ventricular cardiomyocytes using a bioavailable human metabolite derived from berries diet used at physiological concentration.

Berries-enriched diet prolonged the lifespan, maintained the body weight and decreased cardiac and renal hypertrophy of high salt fed rats. These results are consistent with studies showing that berries or pure polyphenols-enriched diets have (direct or systemic) cardioprotective effects in various cardiovascular preclinical models as well as in humans [16,35]. For instance, blueberries have been shown to decrease myocardial infarction, and resveratrol was shown to prevent cardiac remodeling and dysfunction in a model of aortic banded rats [20], in a angiotensin II-induced hypertension model, in spontaneously hypertensive rats (SHR) as well as in a pressure overload mouse model [16,17].

4.1. Beneficial effects of berries against chronic salt consumption

Berries ingestion ameliorated survival, systolic blood pressure (SPB) and cardiac function in HS rats (Fig 1). Likewise, berries decreased LV hypertrophy, improved diastolic function, LV relaxation and a contractility index (Fig 1). Since hypertension is associated with several

comorbidities, such as renal disease and aortic remodeling [22,31-34], it is likely that the beneficial properties of berries ingestion is achieved *via* both systemic and direct cardiac effects of berries components, such as polyphenols and/or their metabolites. Indeed, our *in vivo* data showed that berries decreased renal hypertrophy and dysfunction, which is in agreement with an earlier study showing that blueberries maintained renal hemodynamics and filtration in a SHR rat model [36]. Berries ingestion also normalized the aortic wall cross section and upregulated AQP1 expression (Fig 3). The latter effect represents an important finding since AQP1 is known to facilitate the diffusion of NO out from endothelial cells [34] and into vascular smooth muscle cells [33]. Furthermore, transport of NO by means of AQP1 was shown to control endothelium-dependent relaxation of mouse aortic rings [34]. AQP1 and a series of other members of the aquaporin family of membrane channels also play roles in oxidative stress, cell signaling and aging [35] and are emerging among the targets of bioactive phytochemicals in imparting their beneficial actions [36].The observed improvement of aortic morphology and reduction in SBP upon berries ingestion might thus be associated with endothelium-dependent vascular changes, increased relaxation [39], enhanced eNOS activity and increased NO output [40]. However, other studies found no effect of resveratrol on SBP despite a beneficial effect seen on cardiac hypertrophy [20,41]. While the differences may be due to differences in the experimental temporal window, a direct and specific anti-hypertrophic effect of resveratrol or its metabolites on the heart cannot be discarded.

4.2. The beneficial effects of berries on cardiac hypertrophy and tissue cohesion involve CSRP3

Surprisingly, the beneficial effects of berries were not explained by modulation of cell death, mitochondrial mass, autophagy, or glucose and lipids metabolism since no significant changes in these processes were detected *ex vivo* in the 4 groups of animals tested here (Table Supp 2; Fig 5-6). In contrast, the protective role of berries ingestion was associated with increased myocardial tissue cohesion and contractility, which appeared to be correlated with a decrease in the expression of the mechanosensor and cytoskeleton protein CSRP3 *in*

vivo. While CSRP3 expression was strongly increased in HS diet fed rats, it was decreased back to LS level in HS berries fed rats (Fig 4).

In vitro, primary cardiomyocytes were treated with pure polyphenols, resveratrol and MC, for two hours before 48 h phenylephrine treatment and further analysis (Fig 6). These experiments demonstrate that resveratrol and MC inhibit the CSRP3 overexpression induced by phenylephrine. Mechanistically, it is tempting to speculate that both polyphenols modulate one of several targets belonging to the signaling cascade leading to CSRP3 stabilisation and PE hypertrophic effect. Besides the molecular mechanisms of CSRP3 role are still unclear, changes in CSRP3 expression might affect its interaction with its molecular partners such as α-actinin and telethonin [7] and might modify the cytoarchitecture of the cardiomyocytes. Interestingly, PE was shown earlier to promote the translocation of CSRP3 into the nucleus [42,43] and to increase hypertrophy markers such α-actinin and brain natriuretic peptide (BNP) mRNA [42]. In our hands, no CSRP3 nuclear translocation was detected (not shown) suggesting a novel undescribed mechanism.

4.3. Cellular mechanisms in the cardioprotection conferred by berries consumption

Most of the protective effects of berries are usually attributed to their ability to enhance antioxidant defense [17] by an enhanced expression of the mitochondrial enzyme Mn-superoxide dismutase (SOD2) [44], an increased glutathione levels [45], an activation of eNOS [46,47], a decrease in angiotensin I, II and endothelin 1, as well as a decrease in the circulating renin-angiotensin system activation [48]. Moreover, pure polyphenol compounds such as resveratrol can inhibit hypertrophy response and alter cardiac function in many models of hypertension. Resveratrol effect can be partially due to activation of AMPK and inhibition of PI3K/Akt/mTOR/p70S6 pathway [49], but also via effects on inflammation and a plethora of molecular targets such as SIRT-1 [16], nuclear factor (erythroid-derived 2)-like 2 (Nrf2) [16], and nuclear factor of kappa light polypeptide gene enhancer in B-cells (NFκB) [50]. Likewise, resveratrol may also improve Ca^{2+} cycling through activation of the

sarcoplasmic/endoplasmic reticulum Ca^{2+}-ATPase 2a (SERCA2) expression via SIRT-1 [51] and via inhibition of hypertrophic gene expression. Finally, resveratrol has been linked to autophagy induction through both AMPK and SIRT-1 pathways [16] and to increased mitochondrial biogenesis [52]. Because of the potential pleiotropic effects, it is likely that the beneficial effects of berries ingestion involved multiple signaling pathways acting on a variety of cellular targets.

Our finding showed that polyphenols metabolites derived from berries such MC decreased cardiomyocyte size and regulated CSRP3 expression (Fig 6), results also obtained for resveratrol and that were consistent with previous observations showing that resveratrol reduced PE-induced protein synthesis and cell growth in rat cardiac myocytes [50]. In particular, MC is a polyphenol metabolite detected in the circulation in humans after ingestion of a berries mixture with the same composition as used in this work [19], and may thus represent a potential effector present in our trial. Moreover, it is important to note that, in contrast to numerous studies that used very high doses of pure polyphenols, the doses used in our cellular experiments reflects physiological doses circulating in human [18,19]. Hence, our results might be particularly relevant for human health and can be useful for translational studies.

Global understanding of the molecular response to pathologies, nutrition and/or treatments involves the study of proteome variations at the level of protein expression, localization and post-translational modifications [53]. Here, we focused our study on changes in expression level of proteins postulating that these changes may have an impact on the activity of these proteins and this would lead to the identification of key targets. By 2D DIGE, we identified several spots for CSRP3, Myosin 7 and Major vault protein (Table S6). Thus, it will be important in the future to analyse the potential of berry polyphenols to modify the post-translational modifications to exert their protective effects [53].

5. Conclusion

The Dahl/SS rats constitutes a preclinical chronic model that recapitulates many aspects found in humans suffering from hypertension-induced heart failure [22-23].This model was instrumental to discover novel insights into the cardiac tissue protection conferred by berries based on the evaluation of structural, functional and proteomic data. Combining *in vivo* and cellular findings, we revealed a novel berries-mediated cardioprotective pathway centered on CSRP3-modulation of cardiac hypertrophy and tissue cohesion. This study contributes to promote berries consumption in order to limit deleterious effects of hypertension in humans.

Acknowledgements

The authors wish to thank Pedro Oliveira (Instituto Nacional de Investigação Agrária, Oeiras, Portugal) for providing *Vaccinium* spp., *Rubus* spp. and *R. idaeus* fruits. We also thank Francoise Gaudin for histology staining (UMS-IPSIT). Furthermore, we thank INRA Jouy en Josas for animal diet and Valérie Domergue-Dupont (Animal Core Facility, UMS-IPSIT).

Sources of Funding

CB, CNS, HLAV, CO were funded by ANR (ANR-13-ISV1-0001-01) and FCT (FCT-ANR/BEX-BCM/0001/2013). We also acknowledge the Investment for the Future program ANR-11-IDEX-0003-01 within the LABEX ANR-10-LABX-0033 (CB, CO, RF), Fundação para a Ciência e Tecnologia financial support of AG (SFRH/BD/103155/2014), HLAV (IF/00185/2012) and CNS (IF/01097/2013). iNOVA4Health Research Unit (LISBOA-01-0145-FEDER-007344), which is cofunded by FCT through national funds, and by FEDER under the PT2020 Partnership Agreement, is acknowledged.

Disclosures

The authors have no disclosures to declare.

Author contributions

Carole Oudot conceived the study, performed animal, cellular and molecular experiments, analyzed the data and wrote the paper
Andreia Gomes performed berry preparation and analysis experiments and wrote the paper
Valérie Nicolas performed confocal microscopy experiments and analyzed the data
Morgane Le Gall performed proteomic experiments and analyzed the data
Philippe Chaffey performed proteomic experiments and analyzed the data
Cédric Broussard performed proteomic experiments and analyzed the data
Giuseppe Calamita performed aorta experiments, analyzed the data and wrote the paper
Maria Mastrodonato performed aorta experiments, analyzed the data
Patrizia Gena performed aorta experiments, analyzed the data
Jean-Luc Perfettini provide materials for cellular experiments and analyzed the data
Jocelyne Hamelin performed metabolic experiments and analyzed the data
Antoinette Lemoine performed metabolic experiments and analyzed the data
Rodolphe Fischmeister analyzed the data and wrote the paper
Helena L.A. Vieira conceived the study, analyzed the data and wrote the paper
Claudia N. Santos conceived the study, provide berry materials, analyzed the data, obtained grant support and wrote the paper
Catherine Brenner conceived the study, provided animal, cellular and molecular experiments materials, analyzed the data, supervised the project, obtained grant support and wrote the paper

References

[1] J. He, P.K. Whelton, Epidemiology and prevention of hypertension, Med. Clin. North Am. 81 (1997) 1077–1097. doi:10.1016/S0025-7125(05)70568-X.

[2] M. Kokubo, A. Uemura, T. Matsubara, T. Murohara, Noninvasive evaluation of the time course of change in cardiac function in spontaneously hypertensive rats by echocardiography, Hypertens. Res. 28 (2005) 601–609. doi:10.1291/hypres.28.601.

[3] B.J. Gersh, B.J. Maron, R.O. Bonow, J.A. Dearani, M.A. Fifer, M.S. Link, S.S. Naidu, R.A. Nishimura, S.R. Ommen, H. Rakowski, C.E. Seidman, J.A. Towbin, J.E. Udelson, C.W. Yancy, 2011 ACCF/AHA Guideline for the Diagnosis and Treatment of Hypertrophic Cardiomyopathy: a report of the American College of Cardiology Foundation/American Heart Association Task Force on Practice Guidelines. Developed in collaboration with the American As, J. Am. Coll. Cardiol. 58 (2011) e212-260. doi:10.1016/j.jacc.2011.06.011.

[4] M.L. McCain, K.K. Parker, Mechanotransduction: the role of mechanical stress, myocyte shape, and cytoskeletal architecture on cardiac function, Pflugers Arch. Eur. J. Physiol. 462 (2011) 89–104. doi:10.1007/s00424-011-0951-4.

[5] R.C. Lyon, F. Zanella, J.H. Omens, F. Sheikh, Mechanotransduction in cardiac hypertrophy and failure, Circ. Res. 116 (2015) 1462–1476. doi:10.1161/CIRCRESAHA.116.304937.

[6] C. Ruwhof, L.A. van der, Mechanical stress-induced cardiac hypertrophy: mechanisms and signal transduction pathways, Cardiovasc. Res. 47 (2000) 23–37. doi:https://doi.org/10.1016/S0008-6363(00)00076-6.

[7] D. Fatkin, R.M. Graham, Molecular mechanisms of inherited cardiomyopathies, Physiol. Rev. 82 (2002) 945–980. doi:10.1152/physrev.00012.2002.

[8] S. Arber, J.J. Hunter, J. Ross Jr., M. Hongo, G. Sansig, J. Borg, J.-C. Perriard, K.R. Chien, P. Caroni, MLP-deficient mice exhibit a disruption of cardiac cytoarchitectural organization, dilated cardiomyopathy, and heart failure, Cell. 88 (1997) 393–403. doi:10.1016/S0092-8674(00)81878-4.

[9] B. Buyandelger, K.E. Ng, S. Miocic, I. Piotrowska, S. Gunkel, C.H. Ku, R. Knöll, MLP (muscle

LIM protein) as a stress sensor in the heart, Pflugers Arch. Eur. J. Physiol. 462 (2011) 135–142. doi:10.1007/s00424-011-0961-2.

[10] C. Kuhn, D. Frank, F. Dierck, U. Oehl, J. Krebs, R. Will, L.H. Lehmann, J. Backs, H.A. Katus, N. Frey, Cardiac remodeling is not modulated by overexpression of muscle LIM protein (MLP), Basic Res. Cardiol. 107 (2012) 262. doi:10.1007/s00395-012-0262-8.

[11] C. Geier, K. Gehmlich, E. Ehler, S. Hassfeld, A. Perrot, K. Hayess, N. Cardim, K. Wenzel, B. Erdmann, F. Krackhardt, M.G. Posch, A. Bublak, H. Nägele, T. Scheffold, R. Dietz, K.R. Chien, S. Spuler, D.O. Fürst, P. Nürnberg, C. Özcelik, Beyond the sarcomere: CSRP3 mutations cause hypertrophic cardiomyopathy, Hum. Mol. Genet. 17 (2008) 2753–2765. doi:10.1093/hmg/ddn160.

[12] S. Morimoto, Sarcomeric proteins and inherited cardiomyopathies, Cardiovasc. Res. 77 (2008) 659–666. http://dx.doi.org/10.1093/cvr/cvm084.

[13] L.P. Svetkey, D. Simons-Morton, W.M. Vollmer, L.J. Appel, P.R. Conlin, D.H. Ryan, J. Ard, B.M. Kennedy, Effects of dietary patterns on blood pressure subgroup analysis of the Dietary Approaches to Stop Hypertension (DASH) randomized clinical trial, Arch Intern Med. 159 (1999) 285–293. doi:10.1001/archinte.159.3.285.

[14] P. Kris-Etherton, R.H. Eckel, B. V. Howard, S.S. Jeor, T.L. Bazzarre, Lyon Diet Heart Study, Circulation. 103 (2001) 1823–1825. doi:10.1161/01.CIR.103.13.1823.

[15] A.M. Miranda, J. Steluti, R.M. Fisberg, D.M. Marchioni, Association between polyphenol intake and hypertension in adults and older adults: A population-based study in brazil, PLoS One. 11 (2016) e0165791. doi:10.1371/journal.pone.0165791.

[16] M. Abbas, F. Saeed, F. Muhammad Anjum, M. Afzaal, T. Tufail, M.S. Bashir, A. Ishtiaq, S. Hussain, H.A.R. Suleria, Natural polyphenols: An overview. International Journal of Food Properties. 20 (2017) 1689-1699

[17] C.N. Santos, A. Gomes, C. Oudot, D. Dias-Pedroso, A Rodriguez-Mateos, H.L.A.Vieira , C. Brenner. Pure Polyphenols Applications for Cardiac Health and Disease. Curr Pharm Des. 24(2018):21372156.doi:10.2174/1381612824666180608102344.

[18] R.C. Pimpão, T. Dew, M.E. Figueira, G.J. Mcdougall, D. Stewart, R.B. Ferreira, C.N. Santos, G. Williamson, Urinary metabolite profiling identifies novel colonic metabolites and conjugates of phenolics in healthy volunteers, Mol. Nutr. Food Res. 58 (2014) 1414–1425. doi:10.1002/mnfr.201300822.

[19] R.C. Pimpão, M.R. Ventura, R.B. Ferreira, G. Williamson, C.N. Santos, Phenolic sulfates as new and highly abundant metabolites in human plasma after ingestion of a mixed berry fruit purée, Br. J. Nutr. 113 (2015) 454–463. doi:https://doi.org/10.1017/S0007114514003511.

[20] S.J. Thandapilly, P. Wojciechowski, J. Behbahani, X.L. Louis, L. Yu, D. Juric, M.A. Kopilas, H.D. Anderson, T. Netticadan, Resveratrol prevents the development of pathological cardiac hypertrophy and contractile dysfunction in the SHR without lowering blood pressure, Am. J. Hypertens. 23 (2010) 192–196. doi:10.1038/ajh.2009.228.

[21] V. Chan, A. Fenning, A. Iyer, A. Hoey, L. Brown, Resveratrol improves cardiovascular function in DOCA-salt hypertensive rats, Curr. Pharm. Biotechnol. 12 (2011) 429–436. doi:10.2174/138920111794480552.

[22] T. Eisenberg, M. Abdellatif, S. Schroeder, U. Primessnig, S. Stekovic, T. Pendl, A. Harger, J. Schipke, A. Zimmermann, A. Schmidt, M. Tong, C. Ruckenstuhl, C. Dammbrueck, A.S. Gross, V. Herbst, C. Magnes, G. Trausinger, S. Narath, A. Meinitzer, Z. Hu, A. Kirsch, K. Eller, D. Carmona-Gutierrez, S. Büttner, F. Pietrocola, O. Knittelfelder, E. Schrepfer, P. Rockenfeller, C. Simonini, A. Rahn, M. Horsch, K. Moreth, J. Beckers, H. Fuchs, V. Gailus-Durner, F. Neff, D. Janik, B. Rathkolb, J. Rozman, M.H. de Angelis, T. Moustafa, G. Haemmerle, M. Mayr, P. Willeit, M. von Frieling-Salewsky, B. Pieske, L. Scorrano, T. Pieber, R. Pechlaner, J. Willeit, S.J. Sigrist, W.A. Linke, C. Mühlfeld, J. Sadoshima, J. Dengjel, S. Kiechl, G. Kroemer, S. Sedej, F. Madeo, Cardioprotection and lifespan extension by the natural polyamine spermidine, Nat. Med. 22 (2016) 1428–1438. doi:10.1038/nm.4222.

[23] S.A. Doggrell, L. Brown, Rat models of hypertension, cardiac hypertrophy and failure,

Cardiovasc. Res. 39 (1998) 89–105. doi:https://doi.org/10.1016/S0008-6363(98)00076-5.

[24] R.C. Pimpão, T. Dew, P.B. Oliveira, G. Williamson, R.B. Ferreira, C.N. Santos, Analysis of phenolic compounds in Portuguese wild and commercial berries after multienzyme hydrolysis, J. Agric. Food Chem. 61 (2013) 4053–4062. doi:10.1021/jf305498j.

[25] Z. Chao, T. Liuyang, L. Nan, C. Qi, C. Zhongqi, L. Yang, L. Yuqi, Mitochondrial tRNA mutation with high-salt stimulation on cardiac damage: underlying mechanism associated with change of Bax and VDAC, Am. J. Physiol. Heart Circ. Physiol. 311 (2016) H1248–H1257. doi:10.1152/ajpheart.00874.2015.

[26] P.M. Becher, F. Gotzhein, K. Klingel, F. Escher, S. Blankenberg, D. Westermann, D. Lindner, Cardiac function remains impaired despite reversible cardiac remodeling after acute experimental viral myocarditis, J. Immunol. Res. 2017 (2017). doi:10.1155/2017/6590609.

[27] H chen, J Yin, Y Deng, M Yang, L Xu, F Teng, D Li, Y Cheng, S Liu, D Wang, T Zhang, W Wu, X Liu, S Guan, B Jiang, G Guo, The protective effects of ginsenoside Rg1 against hypertension target-organ damage in spontaneously hypertensive rats. BMC Complement. Altern. Med. (2012) 12:53 doi.org/10.1186/1472-6882-12-53.

[28] E. Morel, A. Marcantoni, M. Gastineau, R. Birkedal, F. Rochais, A. Garnier, A.-M. Lompré, G. Vandecasteele, F. Lezoualc'h, cAMP-binding protein Epac induces cardiomyocyte hypertrophy, Circ. Res. 97 (2005) 1296–1304. doi:10.1161/01.RES.0000194325.31359.86.

[29] Y. Mallat, E. Tritsch, R. Ladouce, D.L. Winter, B. Friguet, Z. Li, M. Mericskay, Proteome Modulation in H9c2 Cardiac Cells by microRNAs miR-378 and miR-378, Mol. Cell. Proteomics. 13 (2014) 18–29. doi:10.1074/mcp.M113.030569.

[30] A. Shevchenko, H. Tomas, J. Havli, J. V Olsen, M. Mann, In-gel digestion for mass spectrometric characterization of proteins and proteomes, Nat. Protoc. 1 (2007) 2856. http://dx.doi.org/10.1038/nprot.2006.468.

[31] J.W. Gu, A.P. Bailey, W. Tan, M. Shparago, E. Young, Long-term high-salt diet causes hypertension and decreases renal expression of vascular endothelial growth factor in Sprague-Dawley rats, J. Am. Soc. Hypertens. 2 (2008) 275–285. doi:10.1016/j.jash.2008.03.001.

[32] M. Metra, G. Cotter, M. Gheorghiade, L. Dei Cas, A.A. Voors, The role of the kidney in heart failure, Eur. Heart J. 33 (2012) 2135–2142. doi:10.1093/eurheartj/ehs205.

[33] M. Herrera, N.J. Hong, J.L. Garvin, Aquaporin-1 transports NO across cell membranes, Hypertension. 48 (2006) 157–164. doi:10.1161/01.HYP.0000223652.29338.77.

[34] M. Herrera, J.L. Garvin, Novel role of AQP-1 in NO-dependent vasorelaxation, Am. J. Physiol. Renal Physiol. 292 (2007) F1443-1451. doi:10.1152/ajprenal.00353.2006.

[35] G. Tamma, G. Valenti, E. Grossini, S. Donnini, A. Marino, RA. Marinelli, G. Calamita, Aquaporin Membrane Channels in Oxidative Stress, Cell Signaling, and Aging: Recent Advances and Research Trends. Oxid Med Cell Longev. 2018 (2018) 1501847. doi: 10.1155/2018/1501847. eCollection 2018.

[36] A. Tesse, E. Grossini, G.Tamma G, C. Brenner, P. Portincasa, RA. Marinelli, G. Calamita, Aquaporins as Targets of Dietary Bioactive Phytocompounds. Front Mol Biosci. 5 (2018) 30. doi: 10.3389/fmolb.2018.00030

[36] A. Rodriguez-Mateos, C. Heiss, G. Borges, A. Crozier, Berry (poly)phenols and cardiovascular health, J. Agric. Food Chem. 62 (2014) 3842–3851. doi:10.1021/jf403757g.

[37] C.M. Elks, S.D. Reed, N. Mariappan, B. Shukitt-Hale, J.A. Joseph, D.K. Ingram, J. Francis, A blueberry-enriched diet attenuates nephropathy in a rat model of hypertension via reduction in oxidative stress, PLoS One. 6 (2011) e24028. doi:10.1371/journal.pone.0024028.

[38] D. Bonnefont-Rousselot, Resveratrol and Cardiovascular Diseases, Nutrients. 8 (2016). doi:10.3390/nu8050250.

[39] R. Miatello, M. Vázquez, N. Renna, M. Cruzado, A.P. Zumino, N. Risler, Chronic administration of resveratrol prevents biochemical cardiovascular changes in fructose-fed rats, Am. J. Hypertens. 18 (2005) 864–870. doi:10.1016/j.amjhyper.2004.12.012.

[40] H. Matsuoka, M. Nakata, K. Kohno, Y. Koga, G. Nomura, H. Toshima, Chronic - arginine

administration attenuates cardiac hypertrophy in spontaneously hypertensive rats, Hypertens. (Dallas, Tex. 1979). 27 (2016) 1–12. doi:https://doi.org/10.1161/01.HYP.27.1.14.

[41] S.Y. Boateng, R.J. Belin, D.L. Geenen, K.B. Margulies, J.L. Martin, M. Hoshijima, P.P. de Tombe, B. Russell, Cardiac dysfunction and heart failure are associated with abnormalities in the subcellular distribution and amounts of oligomeric muscle LIM protein, Am. J. Physiol. Circ. Physiol. 292 (2007) H259–H269. doi:10.1152/ajpheart.00766.2006.

[42] S.Y. Boateng, S.E. Senyo, L. Qi, P.H. Goldspink, B. Russell, Myocyte remodeling in response to hypertrophic stimuli requires nucleocytoplasmic shuttling of muscle LIM protein, J. Mol. Cell. Cardiol. 47 (2009) 426–435. doi:10.1016/j.yjmcc.2009.04.006.

[43] M. Tanno, A. Kuno, T. Yano, T. Miura, S. Hisahara, S. Ishikawa, K. Shimamoto, Y. Horio, Induction of manganese superoxide dismutase by nuclear translocation and activation of SIRT1 promotes cell survival in chronic heart failure, J Biol Chem. 285 (2010) 8375–8382. doi:M109.090266 [pii]\r10.1074/jbc.M109.090266.

[44] D. McCormack, D. McFadden, A review of pterostilbene antioxidant activity and disease modification, Oxid. Med. Cell. Longev. 2013 (2013). 575482-97. doi:10.1155/2013/575482.

[45] T. Wallerath, G. Deckert, T. Ternes, H. Anderson, H. Li, K. Witte, U. Forstermann, Resveratrol, a polyphenolic phytoalexin present in red wine, enhances expression and activity of endothelial nitric oxide synthase, Circulation. 106 (2002) 1652–1658. doi:10.1161/01.CIR.0000029925.18593.5C.

[46] J.F. Leikert, T.R. Rathel, P. Wohlfart, V. Cheynier, A.M. Vollmar, V.M. Dirsch, Red wine polyphenols enhance endothelial nitric oxide synthase expression and subsequent nitric oxide release from endothelial cells, Circulation. 106 (2002) 1614–1617. doi:10.1161/01.CIR.0000034445.31543.43.

[47] M.C. Lazzè, R. Pizzala, P. Perucca, O. Cazzalini, M. Savio, L. Forti, V. Vannini, L. Bianchi, Anthocyanidins decrease endothelin-1 production and increase endothelial nitric oxide synthase in human endothelial cells, Mol. Nutr. Food Res. 50 (2006) 44-51. doi:10.1002/mnfr.200500134.

[48] W. Parichatikanond, D. Pinthong, S. Mangmool, Blockade of the renin-angiotensin system with delphinidin, cyanin, and quercetin, Planta Med. 78 (2012) 1626–1632. doi:10.1055/s-0032-1315198.

[49] A.Y.M. Chan, V.W. Dolinsky, C.-L.M. Soltys, B. Viollet, S. Baksh, P.E. Light, J.R.B. Dyck, Resveratrol inhibits cardiac hypertrophy via AMP-activated protein kinase and Akt, J. Biol. Chem. 283 (2008) 24194–24201. doi:10.1074/jbc.M802869200.

[50] K. Ashikawa, S. Majumdar, S. Banerjee, A.C. Bharti, S. Shishodia, B.B. Aggarwal, Piceatannol Inhibits TNF-Induced NF-κB Activation and NF-κB-Mediated Gene Expression Through Suppression of IκBα Kinase and p65 Phosphorylation, J. Immunol. 169 (2002) 6490–6497. doi:https://doi.org/10.4049/jimmunol.169.11.6490.

[51] M. Sulaiman, M.J. Matta, N.R. Sunderesan, M.P. Gupta, M. Periasamy, M. Gupta, Resveratrol, an activator of SIRT1, upregulates sarcoplasmic calcium ATPase and improves cardiac function in diabetic cardiomyopathy, Am. J. Physiol. Heart Circ. Physiol. 298 (2010) H833-843. doi:10.1152/ajpheart.00418.2009.

[52] Z. Ungvari, W.E. Sonntag, R. de Cabo, J.A. Baur, A. Csiszar, Mitochondrial protection by resveratrol, Exerc. Sport Sci. Rev. 39 (2011) 128–132. doi:10.1097/JES.0b013e3182141f80.

[53] AR Wende, Post-translational modifications of the cardiac proteome in diabetes and heart failure. Proteomics Clin. App. 10 (2016) 25-38.

Legends to Figures

Fig. 1 Berries improve rat survival, body weight, blood pressure and cardiac performance. A, Flow chart of the trial. A berries mixture was supplemented or not in the food to LS diet rats (LS and LS Berries) and HS diet rats (HS and HS Berries) for 10 weeks**. B,** Kaplan–Meier survival analysis for N=6 LS, N=6 LS Berries, N=14 HS, N=14 HS Berries, (logrank test: Chi2:10.1, df: 3, p<0.05) **C,** Serial data on body weight. Data represent mean±SEM. *p<0.05 *vs* LS; $ p<0.05 *vs* LS Berries; † p<0.05 *vs* HS. N=6 LS, N=6 LS Berries, N=8 HS, N=13 HS Berries. **D,** Systolic blood pressure (SBP) measurement by tail cuff method. Data represent mean±SEM. *p<0.05 *vs* LS; $ p<0.05 *vs* LS Berries; † p<0.05 *vs* HS. N=6 LS, N=6 LS Berries, N=8 HS. N=13 HS Berries. **E**, Representative M-mode images of the left ventricle (LV) in LS, LS Berries, HS, and HS Berries groups after 9 weeks. Graph of LV end systolic diameter, graph of LV fractional shortening and graph of calculated LV mass indexed by tibia length. Data represent mean±SEM, N= 5 LS, N=5 LS Berries, N=8 HS, N=12 HS Berries. *p<0.05 vs LS; $ p<0.05 vs LS Berries; † p<0.05 vs HS.

LV, left ventricle; N, number of rats.

Fig 2. Left ventricle tissue alterations and berries-induced protection. A, Hematoxylin-eosin staining on LV sections with cardiomyocytes area quantification (Magnification x50). **B,** LV on endocardium sections with semi-quantitative quantification for desarcomerization (Arrows: desarcomerization) Data represent % images according to 3 categories (No desarcomerization, Minimal desarcomerization, Moderate to severe desarcomerization) performed on N=5 rats/group. (Chi 2: 14.9; dl 4; $p<0.001$)**.** Test performed to compare group according categories *$p<0.05$ *vs* LS group; † $p<0.05$ *vs* HS group. (Chi 2: 26.7; dl 4; $p<0.001$). **C,** LV on epicardium sections with semi-quantitative quantification for inflammation (Arrows: inflammation marks) Data represent % images according to 3 categories (No inflammation, Minimal inflammation, Moderate to severe inflammation) performed on N=5 rats/group. (Chi 2: 14.9; dl 4; $p<0.001$)**.** Test performed to compare group according categories *$p<0.05$ *vs* LS group; † $p<0.05$ *vs* HS group. **D,** Trichrome Masson staining with fibrosis quantification in the vessels and interstice. Collagen was measured by color-deconvolution of images from Masson-trichrome stained LV sections. Threshold in Image J was applied. Area percentage of collagen was obtained by division of the combined image by the total tissue image. (Magnification x 25). Data represent mean±SEM. N=5 rats/group. *$p<0.05$ *vs* LS; † $p<0.05$ *vs* HS.

Fig. 3 Berries protected the aorta and regulate AQP1 expression. A, Sirius staining on aorta section and **B,** aortic cross section area quantification. Magnification x3.5. **C,** Berries restored aquaporin the endothelial expression of AQP1 which was decreased in HS rats. Sections (6 µm thick) of rat aorta were submitted to immunoperoxidase (panels I, III and V; brown staining; black arrows) or immunofluorescence (panels II, IV and VI; green staining; white arrows) labeling for AQP1. I and II, sections of LS rats. III and IV, sections from HS rats. V and VI, sections from HS Berries rats. Scale bars: 25 µm. TI, tunica intima; TM, tunica media; SM, smooth muscle. N=5 rats/group. *$p<0.05$ vs LS; † $p<0.05$ vs HS Berries.

Fig. 4 Proteomic analysis of left ventricle tissue in Dahl/SS from LS, LS Berries, HS and HS Berries. A, Workflow for identification of targets and validation strategy. **B,** Principal component analysis (each dot represents the proteome map of one sample) and hierarchical clustering of the 52 differentially expressed spots identified. **C,** Representative image of 2D-DIGE analytical gel of cardiac LV labeled and separated by 2D-electrophoresis as described in Materials and Methods. Surrounded spots correspond to the 52 differentially expressed spots detected and identified in at least one of the following comparisons; HS *vs* HS Berries, HS *vs* LS or LS Berries *vs* LS. Black surrounding corresponds to spots differentially expressed between HS and HS Berries. N= 3 rats per group. and **D,** Representative Western blots for CSRP3 and quantification using GAPDH as a loading control. Data represent mean±SEM. **p*<0.05 *vs* LS; † *p*<0.05 *vs* HS.

Fig. 5. Mitochondrial mass was not changed in cardiomyocytes of HS berries rats. A, Citrate synthase activity was performed on left ventricle homogenate from Dahl/SS rats (N=6 rats/group). Experiment was performed in duplicate**. B,** Left ventricle extract (50 µg) from Dahl/SS rats were used for western blot of cytochrome *c*. **C,** Representative western blots for AIF and **D,** for Beclin 1 and LC3 I/II. GAPDH is used as a loading control. Data represent mean±SEM. **p*<0.05 *vs* LS; † *p*<0.05 *vs* HS.

Fig. 6 CSRP3 siRNA and 4-methylcatechol sulfate modulate cell hypertrophy induced by phenylephrine (PE). A, Representative Western blots for α-actinin, CSRP3, GAPDH and respective quantification for neonatal rat ventricular cardiomyocytes (NRVC) treated with 80 nM CSRP3 siRNA effect (n=3 experiments) and 50 µmol/L of PE. **B,** Confocal Immunofluorescence experiments using calcein staining showing cardiomyocyte size (Magnification x83 with 0.8 µm optical slice thickness), and quantification of cell volume area in cardiomyocytes (n=3 experiments with at least 30 cells/group). **C,** Immunofluorescence experiments using α-actinin sarcomeric antibody showing attenuated sarcomerogenesis with siRNA CSRP3 (Magnification x 63). **D**, Representative Western-blots for CSRP3, GAPDH, α-

actinin and respective quantification for NRVC treated for 2h with MC at 1, 5 or 10 μmol/L followed by 24h treatment with 50 μmol/L of PE. **E,** Representative Western-blots for CSRP3, GAPDH and respective quantification for NRVC treated for 2h with 5 and 10 μmol/L of Resveratrol, followed by 24h treatment with 50 μmol/L of PE. Co, control cells; Co-lip, cells with lipofectamine corresponding to siRNA control, CSRP3 si, siRNA CSRP3. n=3 experiments. Data represent mean±SEM. *$p<0.05$ vs Co; $ $p<0.05$ vs CSRP3 si. † $p<0.05$ vs PE.

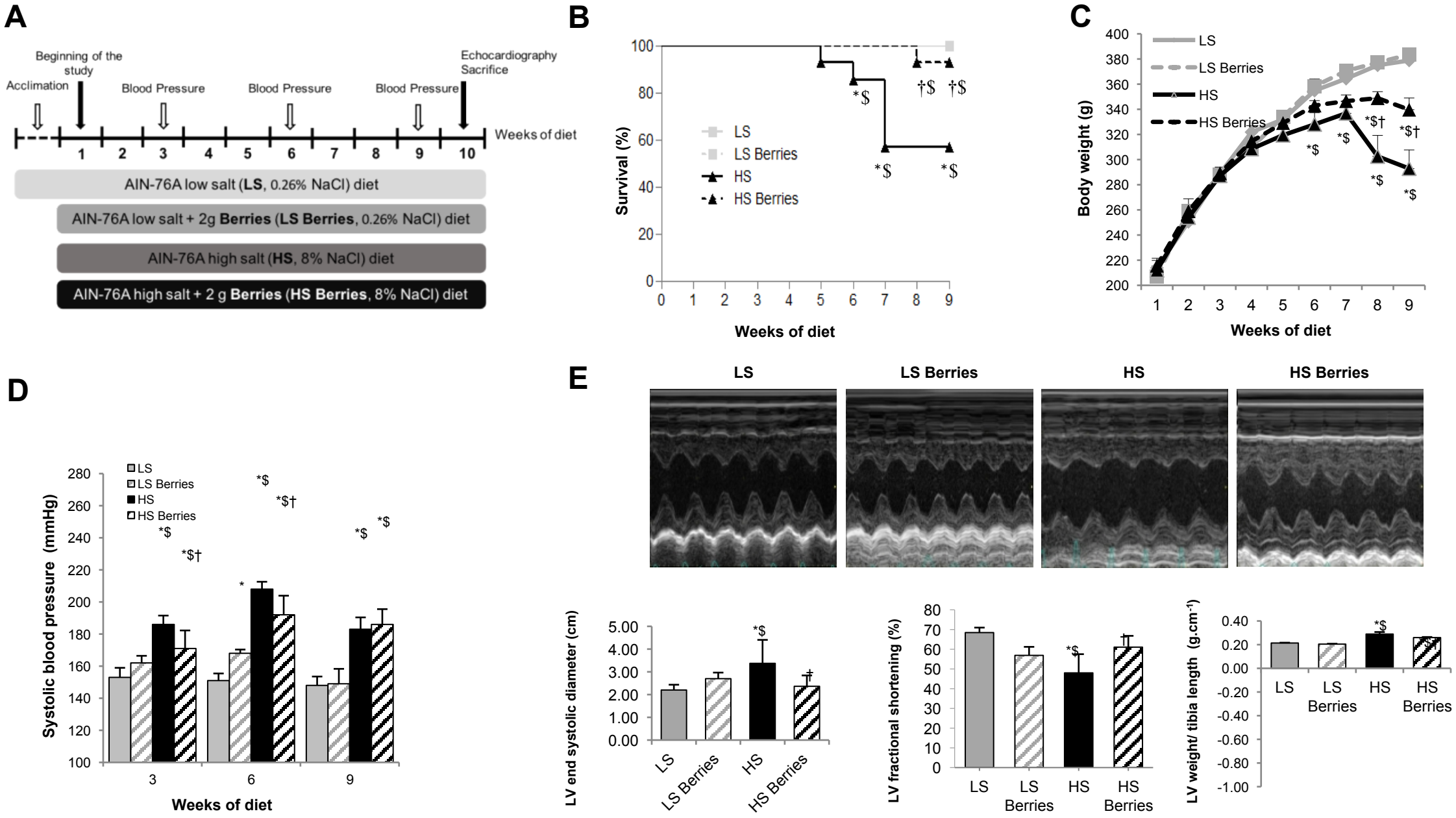
A
Beginning of the study
Acclimation
Blood Pressure
Blood Pressure
Blood Pressure
Echocardiography
Sacrifice
Weeks of diet
1 2 3 4 5 6 7 8 9 10
AIN-76A low salt (LS, 0.26% NaCl) diet
AIN-76A low salt + 2g Berries (LS Berries, 0.26% NaCl) diet
AIN-76A high salt (HS, 8% NaCl) diet
AIN-76A high salt + 2 g Berries (HS Berries, 8% NaCl) diet
B
Survival (%)
LS
LS Berries
HS
HS Berries
Weeks of diet
C
Body weight (g)
LS
LS Berries
HS
HS Berries
Weeks of diet
D
Systolic blood pressure (mmHg)
LS
LS Berries
HS
HS Berries
Weeks of diet
E
LS
LS Berries
HS
HS Berries
LV end systolic diameter (cm)
LV fractional shortening (%)
LV weight/ tibia length (g.cm-1)

Fig. 1

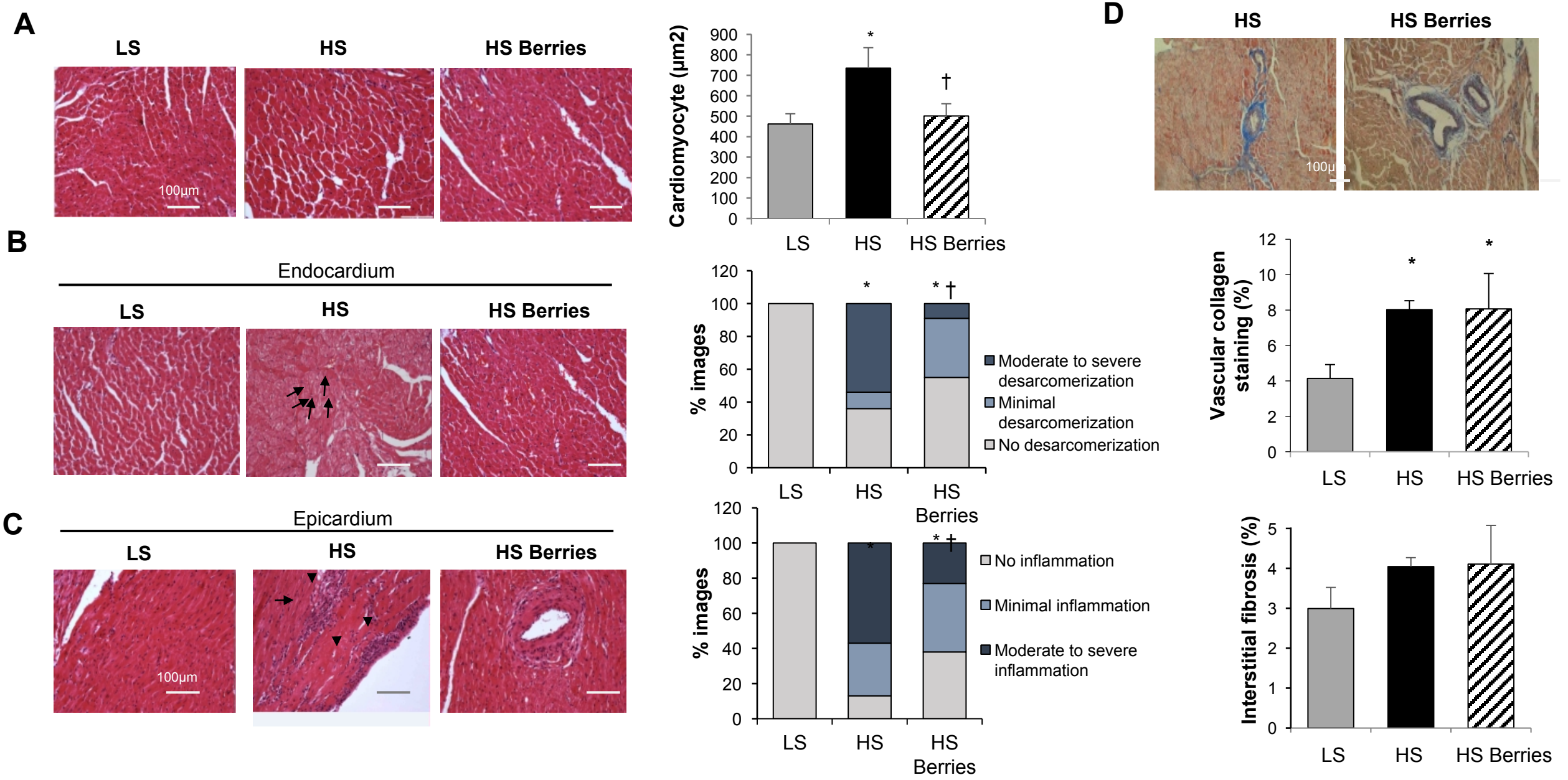
A
LS
HS
HS Berries
100µm
B
Endocardium
LS
HS
HS Berries
C
Epicardium
LS
HS
HS Berries
100µm
Cardiomyocyte (µm2)
900
800
700
600
500
400
300
200
100
0
*
†
LS
HS
HS Berries
% images
120
100
80
60
40
20
0
*
* †
Moderate to severe desarcomerization
Minimal desarcomerization
No desarcomerization
LS
HS
HS Berries
% images
120
100
80
60
40
20
0
*
* †
No inflammation
Minimal inflammation
Moderate to severe inflammation
LS
HS
HS Berries
D
HS
HS Berries
100µm
Vascular collagen staining (%)
12
10
8
6
4
2
0
*
*
LS
HS
HS Berries
Interstitial fibrosis (%)
5
4
3
2
1
0
LS
HS
HS Berries

Fig. 2

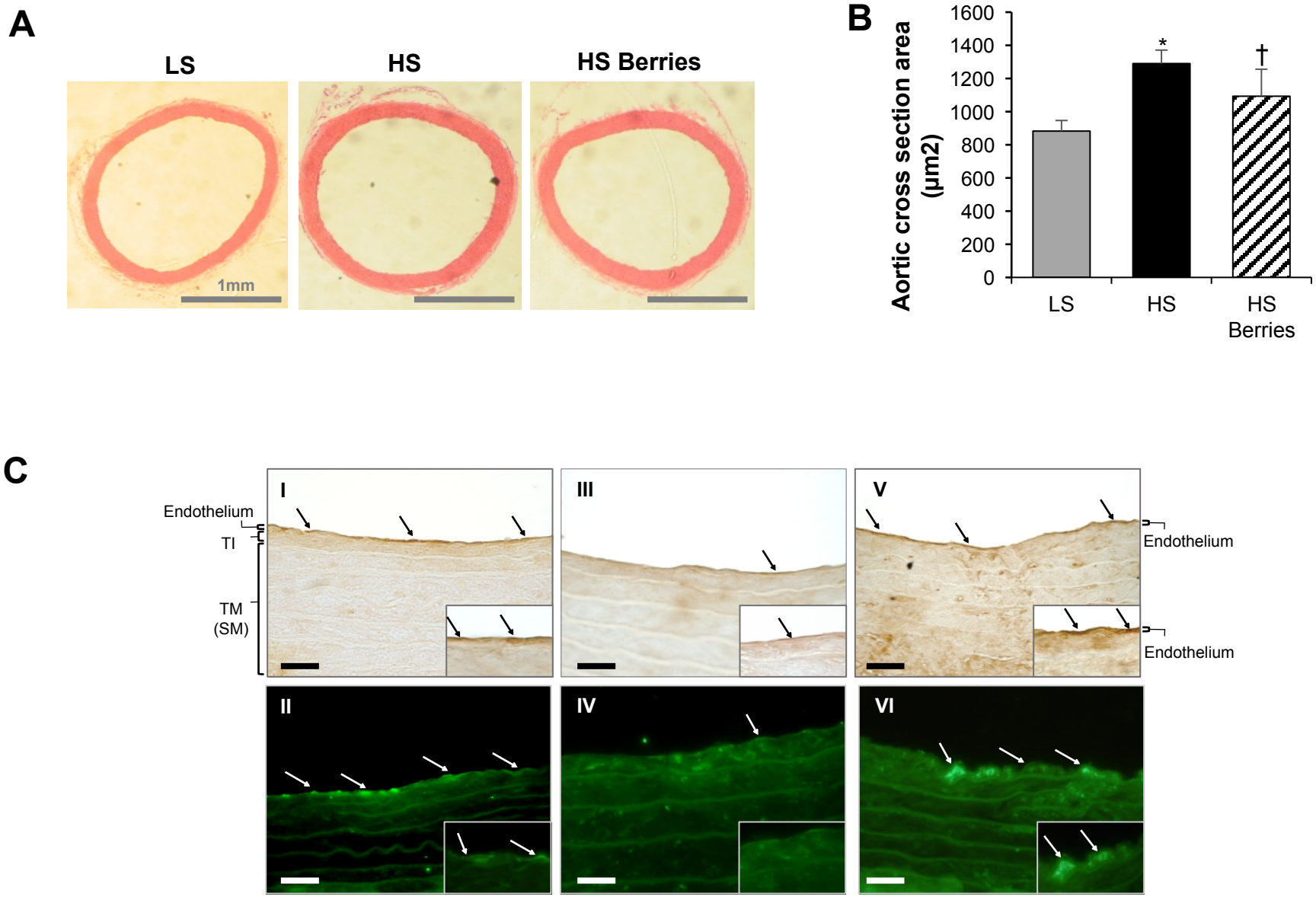
A
LS
HS
HS Berries
1mm
B
Aortic cross section area (µm2)
1600
1400
1200
1000
800
600
400
200
0
*
†
LS
HS
HS Berries
C
Endothelium
TI
TM (SM)
I
III
V
Endothelium
Endothelium
II
IV
VI

Fig. 3

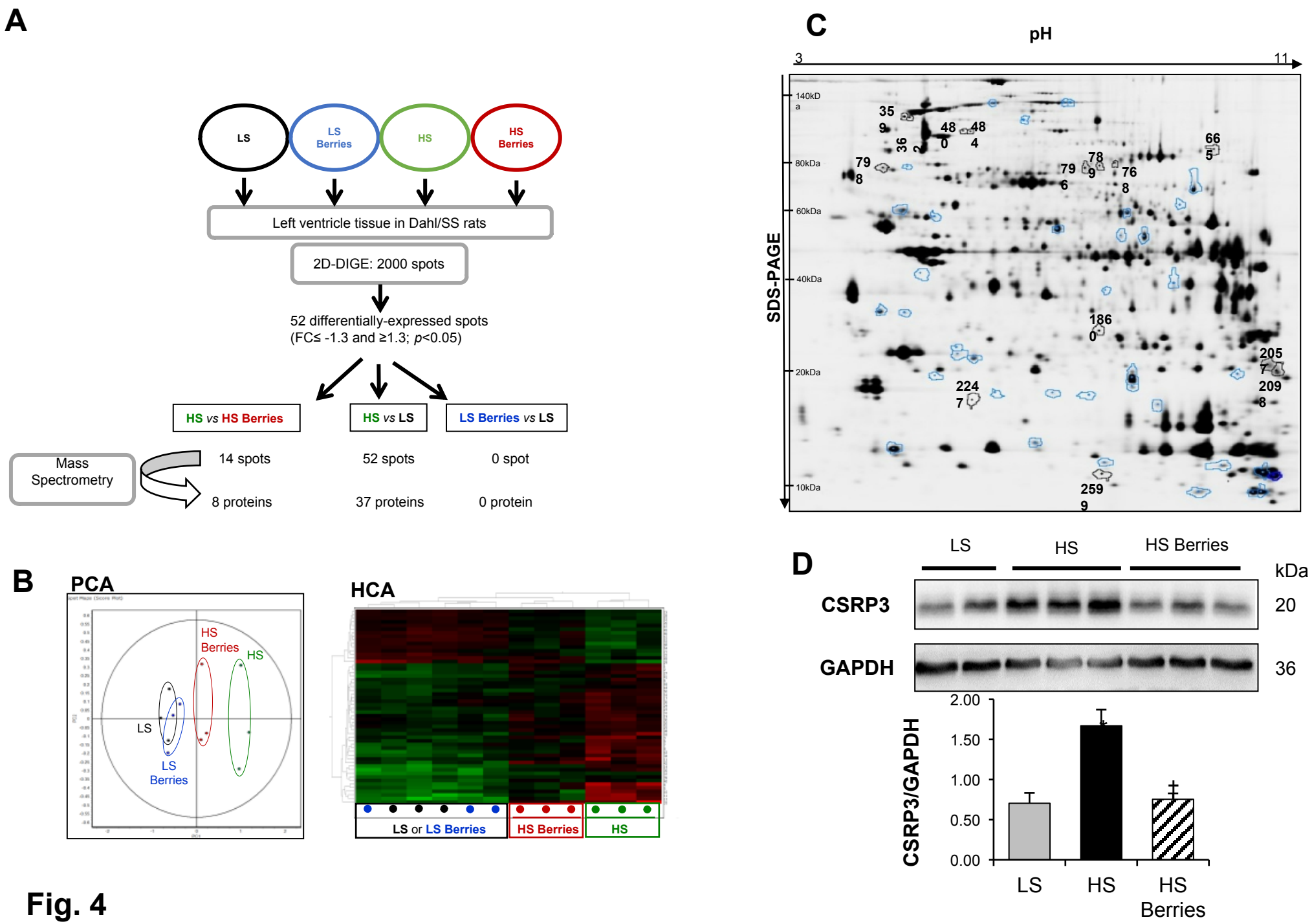
A
LS
LS Berries
HS
HS Berries
Left ventricle tissue in Dahl/SS rats
2D-DIGE: 2000 spots
52 differentially-expressed spots
(FC≤ -1.3 and ≥1.3; p<0.05)
HS vs HS Berries
HS vs LS
LS Berries vs LS
Mass Spectrometry
14 spots
52 spots
0 spot
8 proteins
37 proteins
0 protein
B
PCA
HCA
HS Berries
HS
LS
LS Berries
LS or LS Berries
HS Berries
HS
C
pH
3
11
SDS-PAGE
140kDa
80kDa
60kDa
40kDa
20kDa
10kDa
D
LS
HS
HS Berries
kDa
CSRP3
20
GAPDH
36
CSRP3/GAPDH
2.00
1.50
1.00
0.50
0.00
LS
HS
HS Berries

Fig. 4

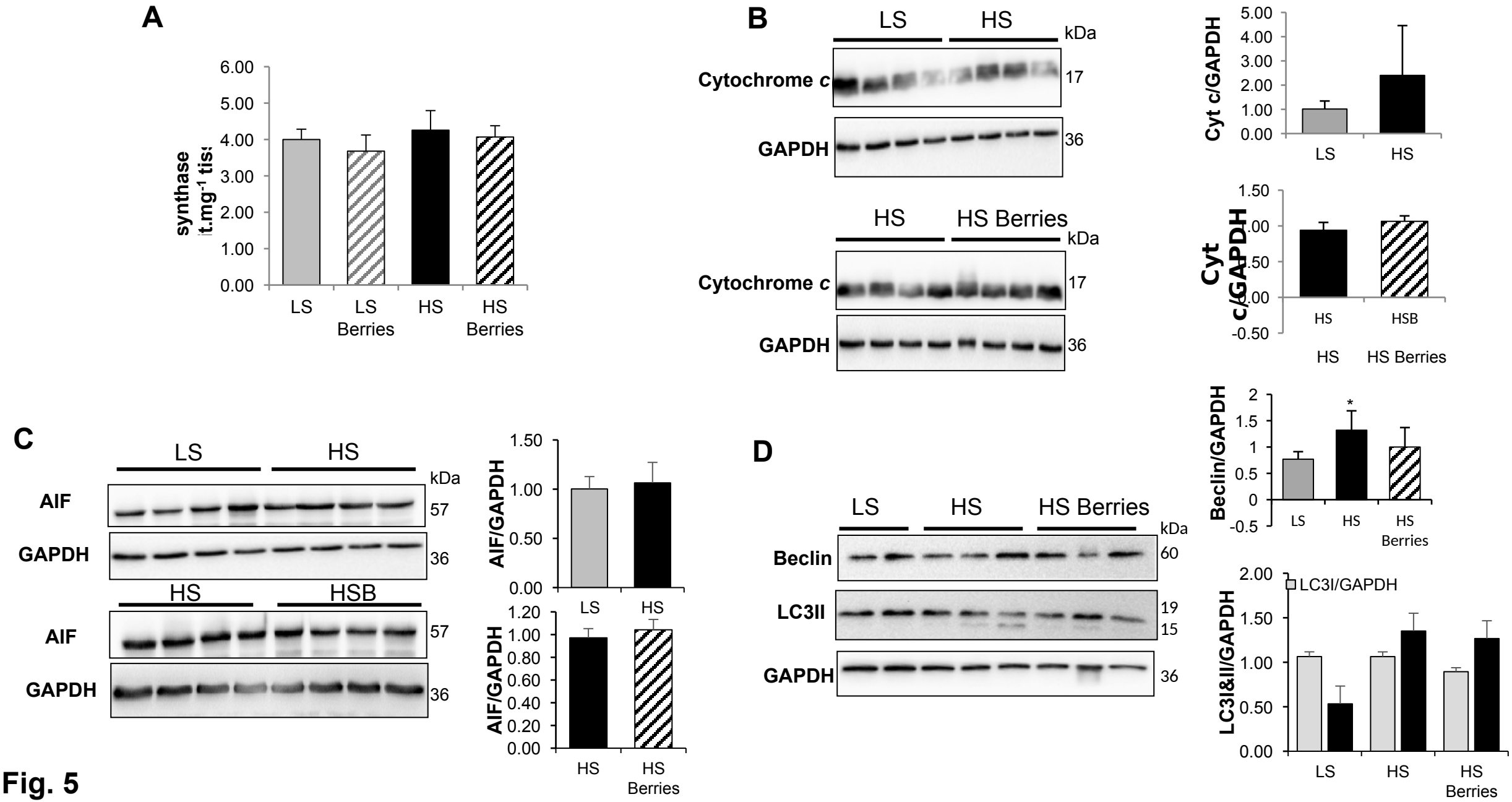
A
synthase
6.00
5.00
4.00
3.00
2.00
1.00
0.00
LS
LS Berries
HS
HS Berries
B
LS
HS
kDa
Cytochrome c
17
GAPDH
36
HS
HS Berries
kDa
Cytochrome c
17
GAPDH
36
Cyt c/GAPDH
5.00
4.00
3.00
2.00
1.00
0.00
LS
HS
Cyt c/GAPDH
1.50
1.00
0.50
0.00
-0.50
HS
HSB
HS
HS Berries
C
LS
HS
kDa
AIF
57
GAPDH
36
HS
HSB
AIF
57
GAPDH
36
AIF/GAPDH
1.50
1.00
0.50
0.00
LS
HS
AIF/GAPDH
1.20
1.00
0.80
0.60
0.40
0.20
0.00
HS
HS Berries
D
LS
HS
HS Berries
kDa
Beclin
60
LC3II
19
15
GAPDH
36
Beclin/GAPDH
2
1.5
1
0.5
0
-0.5
*
LS
HS
HS Berries
LC3I/GAPDH
LC3I&II/GAPDH
2.00
1.50
1.00
0.50
0.00
LS
HS
HS Berries

Fig. 5

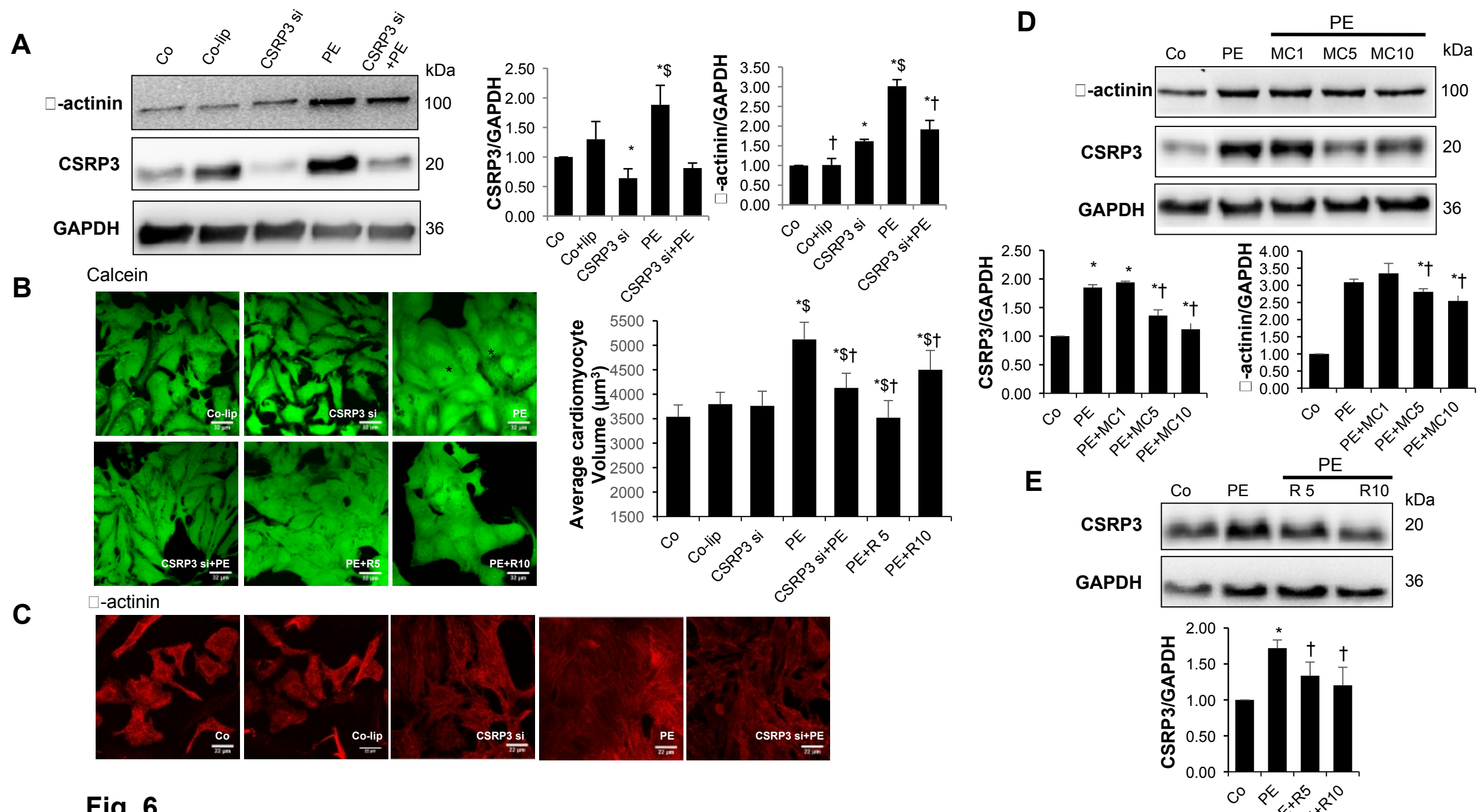
A
Co
Co-lip
CSRP3 si
PE
CSRP3 si +PE
kDa
□-actinin
100
CSRP3
20
GAPDH
36
CSRP3/GAPDH
□-actinin/GAPDH
Co
Co+lip
CSRP3 si
PE
CSRP3 si+PE
B
Calcein
Co-lip
CSRP3 si
PE
CSRP3 si+PE
PE+R5
PE+R10
Average cardiomyocyte Volume (μm³)
C
□-actinin
Co
Co-lip
CSRP3 si
PE
CSRP3 si+PE
D
PE
Co
PE
MC1
MC5
MC10
kDa
□-actinin
CSRP3
GAPDH
100
20
36
CSRP3/GAPDH
□-actinin/GAPDH
PE+MC1
PE+MC5
PE+MC10
E
PE
Co
PE
R 5
R10
kDa
CSRP3
GAPDH
20
36
CSRP3/GAPDH
PE+R5
PE+R10

Fig. 6

Table S1. AIN-76A Diet composition

Ingredients ($g.kg^{-1}$)	LS diet	HS diet
Casein	200	200
Dl-methionine	3	3
Corn starch	150	150
Saccharose	500	423
Cellulose	50	50
Corn oil	50	50
Mineral mix (AIN 76)	35	35
Vitamin mix (AIN 76)	10	10
Choline hydrochloride	2	2
Extra NaCl	0	77

LS: Low Salt

HS: High Salt

Table S3. Echocardiography data

	LS	LS Berries	HS	HS Berries
Heart rate (bpm)	409±28	389± 15	341± 36	380±29
LVDd (mm)	6.40±0.3	6.26±0.26	6.31±0.94	6.03±0.44
LVSd (mm)	2.20±0.23	2.70±0.27	3.10±0.68*$	2.36±0.18†
PWTd (mm)	2.36±0.58	3.03 ±0.50	3.19±0.46*	3.14±0.35*
IVSd (mm)	2.36±0.16	2.04±0.18	2.78±0.43$	2.72±0.31$
RWT	0.7 ±0.1	0.8±0.2	1.1±0.2*$	1.0±0.1*$
LVEF (%)	95±1	90±3	82±9*$	93±3†
Doppler analysis				
E' ($cm.s^{-1}$)	7.1±1.6	7.6±1.3	4.1±0.8*$	6.3±0.9†
E/E'	14.0±3.1	11.3±1.2	17.7±5$	12.5±1.9†

LVDd: left ventricular end diastolic diameter**; LVSd:** left ventricular end systolic diameter**; PWTd:** left ventricular posterior wall thickness**; IVSd:** interventricular septum wall thickness; **RWT:** relative wall thickness; **LVEF:** left ventricule ejection fraction; E': mitral valve annulus velocity; **E:** early diastolic filling on transmitral flow; **E/E':** left ventricular filling pressure. Data are represented as mean ± SEM of values from 5 rats in the LS group and LS Berries group, from 8 rats in HS group and 12 rats in HS Berries group. Statistical differences are denoted as: *p<0.05 *vs* LS; $ p<0.05 *vs* LS Berries; †p<0.05 *vs* HS.

Table S4. Anatomical parameters

	LS	LS Berries	HS	HS Berries
Final BW (g)	379±2	384±5	293±15*$	340±9*$†
Heart weight (g)	1.1±0.04	1.2±0.05	1.4±0.04*$	1.3±0.03*$
Lung weight (g)	1.8±0.13	2.1±0.12	1.7±0.10$	1.6±0.09$
Tibia length (cm)	4.1±0.04	4.2±0.04	3.9±0.03*$	4.0±0.02*$
LV weight (g)	0.9±0.04	0.9±0.04	1.1±0.04*$	1.1±0.03*$†
LV weight /BW ($g.kg^{-1}$ animal)	2.33±0.03	2.27±0.07	3.80±0.14*$	3.18±0.07*$†
Kidney weight (g)	3.0±0.18	3.1±0.18	4.0±0.14*$	3.7±0.12*$†
Kidney weight/BW ($g.kg^{-1}$ animal)	8.0±0.60	8.1±0.59	13.5±0.48*$	11.1±0.40*$†

BW: body weight; **LV:** left ventricle. Data are represented as mean ± SEM of values from 6 rats in the LS group and LS Berries group, from 8 rats in HS group and 12 rats in HS Berries group. *$p<0.05$ *vs* LS; $ $p<0.05$ *vs* LS Berries; †$p<0.05$ *vs* HS.

Table S5. Proteins differentially expressed between HS *vs* LS, HS *vs* HS Berries (HB) and LS *vs* LS Berries (HB). Student t-test p-value and Fold change (Fc) were calculated using DeCyder biological variation module (BVA) module. Grey box: Spot considered as not differentially expressed either because p-value > 0.05 or/and -1.3< Fc > +1.3. [a] Protein name identified by mass spectrometry, [b] Uniprot accession ID

Spot number	Protein name[a]	ACCESSION[b]	HS vs LS		HS vs HB		LS vs LB	
			p-value	Fc	p-value	Fc	p-value	Fc
798	78 kDa glucose-regulated protein	P06761	**5.7E-04**	**2.0**	**5.5E-04**	**1.4**	*2.7E-01*	*-1.1*
1860	Adenylate kinase 2, mitochondrial	P29410	**2.3E-02**	**-2.0**	**1.4E-03**	**-1.9**	*8.3E-01*	*-1.1*
1542	Alpha-1-macroglobulin	Q63041	**7.5E-03**	**1.5**	*5.8E-02*	*1.3*	*1.0E-02*	*-1.1*
2139	Alpha-crystallin B chain	P23928	**3.7E-03**	**1.3**	*2.0E-01*	*1.1*	*6.5E-01*	*-1.0*
2186	Alpha-crystallin B chain	P23928	**1.5E-02**	**1.4**	*3.3E-02*	*1.1*	*9.3E-01*	*-1.0*
1255	Alpha-enolase	P04764	**1.6E-03**	**1.3**	*1.1E-02*	*1.2*	*2.1E-01*	*-1.0*
1620	Annexin A2	Q07936	**1.7E-02**	**1.3**	*4.0E-02*	*1.2*	*4.9E-01*	*-1.1*
1751	Annexin A5	P14668	**2.9E-03**	**1.6**	*2.8E-02*	*1.2*	*3.9E-01*	*-1.1*
2015	Apolipoprotein A-I	P04639	**2.5E-02**	**1.7**	*1.1E-01*	*1.4*	*8.8E-01*	*1.0*
2027	Apolipoprotein A-I	P04639	**8.1E-03**	**2.7**	*1.4E-01*	*1.5*	*3.4E-02*	*1.2*
2596	ATP synthase subunit e & ATP synthase subunit g, mitochondrial	P29419 & Q6PDU7	**8.0E-03**	**-1.4**	*7.1E-02*	*-1.2*	*9.4E-01*	*1.0*
1291	Beta-enolase	P15429	**6.3E-03**	**-1.3**	*2.2E-01*	*-1.1*	*4.4E-01*	*1.1*
1295	Beta-enolase	P15429	**6.4E-03**	**-1.6**	*1.3E-01*	*-1.2*	*2.3E-01*	*1.2*
2269	Cofilin-1	P45592	**4.0E-03**	**1.3**	*1.2E-02*	*1.2*	*4.9E-01*	*-1.1*
2057	CSRP3	P50463	**3.9E-04**	**2.0**	**5.5E-03**	**1.3**	*8.5E-01*	*-1.0*
2098	CSRP3	P50463	**3.9E-03**	**1.9**	**1.8E-02**	**1.3**	*5.9E-01*	*1.1*
2476	Cytochrome c oxidase subunit 5A, mitochondrial	P11240	**5.0E-03**	**-1.7**	*1.1E-01*	*-1.3*	*1.2E-01*	*1.1*
2679	Cytochrome c oxidase subunit 7A2, mitochondrial	P35171	**3.0E-03**	**-1.5**	*1.2E-01*	*-1.2*	*6.2E-02*	*1.1*
2685	Cytochrome c oxidase subunit 7A2, mitochondrial	P35171	**3.5E-03**	**-1.5**	*1.7E-01*	*-1.2*	*2.2E-01*	*1.1*
1145	Desmin	P48675	**2.2E-02**	**1.4**	*2.6E-01*	*1.2*	*8.5E-01*	*-1.0*
1960	Heat shock protein beta-1	P42930	**1.0E-03**	**1.5**	*4.0E-02*	*1.2*	*9.6E-01*	*1.0*
2114	Heat shock protein beta-2	O35878	**6.9E-04**	**1.4**	*4.0E-01*	*1.1*	*9.7E-01*	*-1.0*
2216	Heat shock protein beta-6	P97541	**1.3E-02**	**1.4**	*9.3E-01*	*-1.0*	*7.9E-01*	*-1.0*
2219	Heat shock protein beta-6	P97541	**8.2E-03**	**1.6**	*4.6E-01*	*1.1*	*8.2E-01*	*1.0*
2227	Heat shock protein beta-6	P97541	**2.0E-02**	**1.6**	*3.8E-01*	*-1.1*	*5.4E-01*	*-1.1*
2548	Hemoglobin subunit beta-1	P02091	**1.1E-02**	**-1.4**	*9.5E-02*	*-1.2*	*2.8E-01*	*1.0*
2560	Hemoglobin subunit beta-1	P02091	**2.1E-02**	**-1.6**	*1.4E-01*	*-1.3*	*7.9E-01*	*1.0*
2680	Hemoglobin subunit beta-1	P02091	**1.4E-03**	**-1.4**	*6.6E-02*	*-1.1*	*1.0E-02*	*1.0*
480	Major vault protein	Q62667	**2.5E-03**	**1.8**	**7.5E-03**	**1.4**	*4.0E-01*	*-1.2*
484	Major vault protein	Q62667	**3.8E-03**	**1.9**	**1.4E-02**	**1.5**	*7.6E-01*	*-1.1*
2615	*Myoglobin*	Q9QZ76	**3.6E-03**	**-1.5**	*5.5E-02*	*-1.3*	*4.7E-01*	*1.1*
359	Myosin-6	P02563	**1.3E-03**	**3.1**	**1.3E-02**	**2.1**	*1.0E-01*	*-1.1*
249	Myosin-7	P02564	**2.4E-02**	**1.9**	*1.8E-01*	*1.4*	*3.5E-01*	*-1.1*
362	Myosin-7	P02564	**8.3E-04**	**2.6**	**9.8E-03**	**1.7**	*2.5E-01*	*-1.2*
665	Myosin-7	P02564	**3.4E-03**	**1.7**	**7.3E-03**	**1.5**	*8.8E-01*	*-1.0*
768	Myosin-7	P02564	**2.9E-03**	**2.4**	**3.9E-02**	**1.8**	*2.3E-01*	*-1.2*
789	Myosin-7	P02564	**3.5E-03**	**2.9**	**6.9E-03**	**2.0**	*5.8E-01*	*-1.1*
796	Myosin-7	P02564	**8.8E-04**	**3.4**	**1.0E-02**	**1.9**	*2.2E-01*	*-1.2*
243	Myosin-binding protein C, cardiac-type	P56741	**2.2E-02**	**1.4**	*3.6E-01*	*1.1*	*7.6E-01*	*-1.0*
244	Myosin-binding protein C, cardiac-type	P56741	**2.9E-02**	**1.5**	*4.6E-01*	*1.1*	*8.1E-01*	*-1.0*
792	NADH-ubiquinone oxidoreductase 75 kDa subunit, mitochondrial	Q66HF1	**2.6E-02**	**1.8**	*1.4E-01*	*1.4*	*1.3E-01*	*-1.1*
1631	PDZ and LIM domain protein 1	P52944	**4.4E-03**	**1.4**	*2.2E-02*	*1.1*	*2.0E-01*	*-1.1*
2599	Protein S100-A10	P05943	**9.8E-05**	**1.6**	**2.4E-03**	**1.4**	*1.8E-01*	*-1.1*
1059	Pyruvate kinase PKM	P11980	**2.1E-02**	**1.5**	*1.2E-01*	*1.2*	*4.0E-01*	*-1.1*
1117	Succinyl-CoA:3-ketoacid coenzyme A transferase 1, mitochondrial	B2GV06	**1.6E-02**	**1.3**	*1.3E-01*	*1.1*	*2.3E-01*	*-1.1*
2105	Transgelin-2	Q5XFX0	**2.3E-02**	**1.4**	*1.6E-01*	*1.2*	*1.5E-01*	*-1.2*
2247	Translocon-associated protein subunit delta	Q07984	**7.9E-03**	**2.1**	**5.0E-02**	**1.5**	*3.2E-01*	*-1.1*
2451	Transthyretin	P02767	**8.1E-03**	**-1.5**	*1.6E-01*	*-1.1*	*5.0E-01*	*1.1*
1763	Ubiquinone biosynthesis protein COQ9, mitochondrial	Q68FT1	**5.5E-04**	**-1.4**	*2.8E-03*	*-1.2*	*1.5E-01*	*1.1*
953	Very long-chain specific acyl-CoA dehydrogenase, mitochondria	P45953	**1.8E-03**	**-1.3**	*1.7E-02*	*-1.1*	*3.7E-01*	*1.1*
1086	Vimentin	P31000	**7.0E-03**	**1.5**	*5.9E-02*	*1.2*	*1.1E-01*	*-1.1*
395	Vinculin	P85972	**4.2E-02**	**1.3**	*1.3E-01*	*1.2*	*2.8E-02*	*-1.1*

Table S6. Proteins differentially expressed between HS and HS Berries (HB)

Spot number[a]	Protein name[b]	Accession[c]	HS *vs* HB[d]	Function[e]
1860	Adenylate kinase 2	P29410	-1.9	ATP:AMP phosphotransfer
359	Myosin 6	P2563	2.1	Muscle contraction
362; 665; 768; 789; 796	Myosin 7	P02564	2.6; 1.7; 2.4; 2.9; 3.4	Muscle contraction
480; 484	Major vault protein	Q62667	1.4; 1.5	Nucleo-cytoplasmic transport
2057; 2098	CSRP3	P50463	1.3; 1.3	Myogenesis, myogenic differentiation, mechano sensor protein
2599	Protein S100-A10	P05943	1.4	Cell cycle, cell differentiation, exo/endocytosis
798	78 kDa glucose-regulated protein	P06761	1.4	Endoplasmic reticulum stress
2247	Translocon-associated protein subunit delta	Q07984	1.5	Calcium binding to the endoplasmic reticulum membrane

[a] Spot number refers to Figure 5A

[b] Protein name identified by mass spectrometry

[c] Uniprot accession ID

[d] Fold change calculated using DeCyder biological variation analysis (BVA) module

[e] Biological function indicated by GO database

Table S2. Influence of high salt diet and berries on metabolic and biochemical parameters

	LS	LS Berries	HS	HS Berries
Water intake (mL.day^{-1})	19±4	17±6	58±17*$	61±17*$
Food intake (g)	18±3	21±4	13±6*$	20±6*$†
Sodium intake (mmol.day^{-1})	0.8 ±0.1	0.9 ±0.2	17.5 ±3.6*$	28.9 ±7.6*$†
Creatinuria (mg.day-1)	13±1	12±2	8±1*$	10±1*$†
Renal clearance (ml.min--1gKW-1)	1.0 ±0.1	1.2 ±0.1	0.37±0.07*$	0.49 ±0.08*$†
Urinary volume excretion (mL.day-1)	10±2	10±3	46±17*$	47±10*$
Urinary potassium excretion (mmol.day^{-1})	1.4 ±0.1	1.5 ±0.1	1.1 ±0.1	1.4 ±0.1
Fasting glucose (mg.dL^{-1})	99±7	116±1	98±10	102±8
Cholesterol (mmol.L^{-1})	1.6 ±0.2	1.1 ±0.3	2.4 ±0.9	1.9 ±0.9
Triglycerides (mmol.L^{-1})	0.6 ±0.1	0.5 ±0.1	0.8 ±0.4	0.8 ±0.5

Metabolic parameters are represented as mean ± SEM of values from 6 rats in the LS group and LS Berries group, from 8 rats in HS group and 12 rats in HS Berries group. For fasting glucose, cholesterol and triglycerides measurements, data are represented as mean ± SEM of values from 4 rats by group. *p<0.05 versus LS; $ p<0.05 vs LS Berries; †p<0.05 vs HS. Water intake, urinary excretion of sodium and potassium are expressed as a daily mean value calculated over a 3-day collection period at 9 weeks.